

ELUCIDATING THE RESISTANCE MECHANISM OF
MUROBACTIN ANTIBIOTICS

INVESTIGATION OF A PUTATIVE SELF-RESISTANCE CASSETTE FROM
MUROBACTIN (TYPE V GLYCOPEPTIDE)-PRODUCING BACTERIA

BY: Alexandra Barkhouse, B.Sc.

A Thesis Submitted to the School of Graduate Studies in Partial Fulfilment of the
Requirements for the Degree of Master of Science

McMaster University © Copyright by Alexandra Barkhouse, September 2024

McMaster University

Department of Biochemistry & Biomedical Sciences

Hamilton, Ontario, Canada

MASTER OF SCIENCE (2024)

TITLE: Investigation of a putative self-resistance cassette from muobactin-producing
bacteria

AUTHOR: Alexandra Barkhouse, B.Sc. (Dalhousie University)

SUPERVISOR: Dr. Gerard D. Wright

NUMBER OF PAGES: 83

Lay Abstract

Antibiotics are important tools in modern medicine. Their overuse in the clinic, as well as in agriculture and food production, has decreased their efficacy. Resistance to antibiotics can be acquired from these environments and even derived from antibiotic producers themselves. Understanding antibiotic resistance mechanisms is essential to keeping our antibiotics effective. Murobactins are newly discovered compounds that show activity against Gram-positive bacteria, but no confirmed self-resistance mechanism exists. This research aims to help us understand the function of the putative resistance cassette found in producer strains to combat resistance if these antibiotics were introduced into the clinic. Genes of interest were cloned into susceptible bacterial strains and tested against murobactins, but the strains did not confer resistance and showed no changes in cell shape. These genes may have a different essential function within murobactin producers. Future directions involve making a deletion mutant that contains the murobactin biosynthesis machinery but not the putative resistance genes.

Abstract

Biosynthetic gene clusters (BGCs) encode secondary metabolites, such as antibiotics, which can be produced through bacterial interspecies competition. Cognate resistance genes to the produced antibiotic compounds are typically found within BGCs. Type V glycopeptides – now called murobactins – are a newly characterized sub-class of GPAs that exhibit an unprecedented mechanism of action through the inhibition of cell wall remodelling rather than biosynthesis. However, its cognate resistance cassette has not yet been identified.

A putative cassette is present in several murobactin-producing strains; this is composed of a two-component regulatory system (TCS) homologous to *vanRS*, homologues to the FtsEX ATP-binding cassette family, one protein containing a peptidoglycan-binding domain, and one protein of unknown function. The resistance core lacks the predicted TCS. To confirm that the putative resistance cassette confers resistance to murobactin antibiotics, susceptible hosts were chosen, and constructs containing the resistance core of two murobactin producers and the cassette from one producer were synthesized. The minimum inhibitory concentration (MIC) of the murobactin complestatin was assessed in *Streptomyces* and *Bacillus* species, and there was no change in MIC with the introduction of the putative resistance cassette. Phenotypic analysis of *Streptomyces* species when treated with complestatin did not reveal a distinctive phenotype. When the complestatin resistance core was introduced into *B. subtilis*, there was slight restoration to a healthy phenotype in the presence of complestatin. MICs in murobactin producers, non-producers, and non-producers containing the putative resistance cassette also showed no resistance. As these genes are present across many species, they may contribute to cell division. Developing deletion mutants of these genes within the murobactin biosynthetic gene cluster could aid in understanding the purpose of this gene cluster. This research provides insight into the underlying resistance mechanism utilized by murobactin-producing bacteria and guides engineering approaches that use *Streptomyces* strains for future GPA development and discovery.

Acknowledgements

Looking back on my two years of graduate school, I can understand that what I have done is not an easy feat, but I am glad I took a chance on myself and pursued bigger and better things. I want to thank my supervisor, Dr. Gerry Wright, for taking in a junior scientist who had never played with bacteria before coming to the world-renowned Wright lab. Thank you to my committee members, Dr. Marie Elliot, and Dr. Cameron Currie; I have always enjoyed our committee meetings and appreciated all your thoughtful input about my project.

I want to thank several lab mates who made my experience in the lab just that much better each day. A special thanks to Dr. David Sychantha for teaching me how to work with bacteria for the first time. Thank you for all the pep talks, laughs and every Gen Z slang word of the day. I want to thank Dirk for contributing to this thesis by adding the computational analysis; without you, I would not have all that valuable data. To Jacob, thank you for being the best bench buddy; I will never forget all the laughs, roasting, and the occasional chemistry question, of course. To Divya, thank you for helping me with all things *Streptomyces*, and being there as a listening ear to discuss any problems or experimental results. To Mike, thank you for coming up with the most unconventional experiments to try; I always looked forward to updating you on my progress, especially when the results were positive.

Thank you to my two roommates over the years, Rachel and Amanda. Rachel, I will never forget our Chester's nights watching the newest season of Love is Blind, and I will never forget the support I received from you as a friend and from Frog (Mr. Man) himself. Amanda, I love every fancy dinner we cook for each other, all our trips to Costco and watching Jujutsu Kaisen. Both of you have made Hamilton (Dundas) such a wonderful place to live, and you have given me lifelong friendships.

To my loving partner Aaron, thank you for always supporting me; I would never have been able to get through this without you. You have always been there to help in any way that you can. I am so thankful that my work in Hamilton led me to meet you.

I want to thank my family. To my parents, Tracey, and Laurie, thank you for always believing in me and supporting my dreams. Thank you for picking up every phone call, helping me through any kind of trouble, and cheering me on throughout my Master's degree.

Lastly, I would like to thank my cat, Bea, for being the best pet I could ever hope for. She always knows when something is wrong and is always right there, ready for pets.

Table of Contents	
Lay Abstract	iii
Abstract	iv
Acknowledgements	v
Table of Contents	vi
List of Figures	viii
List of Tables.....	ix
List of Abbreviations	x
Declaration of Academic Achievement	xi
Chapter 1	1
1.0 Introduction: The Investigation of Self-Resistance Mechanisms in Environmental Bacteria Can Alleviate the Antibiotic Resistance Crisis	1
1.1 <i>Streptomyces</i> – the Reservoir of Novel Antibiotics and Novel Resistance Mechanisms	3
1.2 Peptidoglycan Biosynthesis & Remodeling & Peptidoglycan as a Drug Target	6
1.3 Glycopeptide Antibiotics & Resistance	10
1.4 Murobactin Antibiotics & Resistance	13
1.5 Project Objectives	17
Chapter 2: Assessing a putative resistance mechanism using <i>Streptomyces</i> as a host	19
2.1 Introduction.....	19
2.2 Materials & Methods	19
2.2.1 Constructs Made with pIJ10257	19
2.2.2 Conjugation of Plasmids into <i>S. venezuelae</i> and <i>S. coelicolor</i>	20
2.2.3 MICs of Murobactins in <i>Streptomyces</i> and Wright Actinomycetes Collection Strains	21
2.2.4 Assessment of Phenotypic Changes Induced by Murobactin Antibiotics	21
2.2.5 <i>S. venezuelae</i> and <i>S. coelicolor</i> Growth Curves	22
2.2.6 Assessment of Peptidoglycan Biosynthesis	22
2.2.7 Computational Analysis of Putative Resistance Genes	23
2.2.8 RNA Isolation in <i>S. venezuelae</i> and <i>S. coelicolor</i> & cDNA Synthesis	23
2.2.9 RT-qPCR in <i>Streptomyces</i>	24
2.2.10 Sporulation Assay	25
2.2.11 Metagenomic Library Preparation of eDNA with FatI Partial Digestion	25
2.3 Results & Discussion	25
2.3.1 pIJ10257 Constructs.....	25
2.3.2 MICs of Murobactins in <i>Streptomyces</i>	26

2.3.3	Assessment of Phenotypic Changes Induced by Murobactin Antibiotics.....	29
2.3.4	Growth Curves & Assessment of Peptidoglycan Biosynthesis.....	32
2.3.5	Computational Analysis of Putative Resistance Genes	34
2.3.6	RNA Isolation in <i>S. venezuelae</i>	38
2.3.7	RT-qPCR in <i>Streptomyces</i>	39
2.3.8	Sporulation Assay	40
2.3.9	MICs of Murobactins in Wright Actinomycetes Collection strains.....	41
2.3.10	Metagenomic Library Preparation of eDNA with FatI Partial Digestion.....	44
Chapter 3: Assessing a Putative Resistance Mechanism Using <i>B. subtilis</i> as a Host		46
3.1	Introduction.....	46
3.2	Materials & Methods	46
3.2.1	pSWEET Constructs	46
3.2.2	Transformation of <i>B. subtilis</i>	46
3.2.3	MICs of Murobactins in <i>B. subtilis</i>	47
3.2.4	Assessment of Phenotypic Changes Induced by Murobactin Antibiotics	47
3.2.5	Growth Curve of <i>B. subtilis</i> & Assessment of Peptidoglycan Biosynthesis.....	48
3.2.6	RNA Isolation in <i>B. subtilis</i> & cDNA Synthesis	48
3.2.7	RT-qPCR in <i>B. subtilis</i>	48
3.3	Results & Discussion	48
3.3.1	pIJ10257 Constructs.....	48
3.3.2	MICs of Murobactins in <i>B. subtilis</i>	49
3.3.3	Assessment of Cell Shape Changes	50
3.3.4	Growth Curves & Assessment of Peptidoglycan Biosynthesis.....	52
3.3.5	RNA Isolation in <i>B. subtilis</i> & cDNA Synthesis	54
3.3.6	RT-qPCR in <i>B. subtilis</i>	55
3.3.7	Codon Optimization of Putative Resistance Genes for <i>B. subtilis</i>	56
Chapter 4: Conclusions and Future Directions.....		58
Appendices.....		66

List of Figures

Figure 1-1. Illustrated developmental life cycle of <i>Streptomyces</i>	3
Figure 1-2. Simplified scheme of PG biosynthesis.....	7
Figure 1-3. Chemical structure of enugumycin & complestatin.....	12
Figure 1-4. Conserved putative resistance cassette for murobactin antibiotics within producer strain BGCs.....	13
Figure 1-5. The potential mechanism of action for the putative resistance protein complex.....	14
Figure 2-1. Isolated plasmid from positive clones for pIJ10257 constructs containing genes of interest.....	26
Figure 2-2. Light microscopy images from <i>S. coelicolor</i>	30
Figure 2-3. Light microscopy images from <i>S. venezuelae</i> pIJ10257, <i>S. venezuelae</i> pIJ-EnC, <i>S. venezuelae</i> pIJ-Enu, <i>S. venezuelae</i> pIJ-COM.	31
Figure 2-4. Growth curves of <i>Streptomyces</i> in plate reader.....	32
Figure 2-7. Fluorescence microscopy in <i>S. venezuelae</i>	34
Figure 2-8. AlphaFold predictions of EnuPEX complex.....	37
Figure 2-9. Genomic context of putative resistance genes.	38
Figure 2-10. Gels of extracted RNA from <i>S. venezuelae</i>	39
Figure 2-11. RT-qPCR results of pIJ-Enu, pIJ-EnC and pIJ-COM.....	39
Figure 2-12. Sporulation assay on ISP4 and MYM plates.....	41
Figure 2-12. Visualizing partial digestion with FatI.....	44
Figure 3-1. Isolated plasmid from positive clones for pSWEET constructs containing genes of interest.....	49
Figure 3-2. Gram-stained light microscopy images from <i>B. subtilis</i> pSWEET-bgaB and <i>B. subtilis</i> pSWEET-COM	51
Figure 3-3. Light microscopy images from <i>B. subtilis</i> pSWEET-bgaB and <i>B. subtilis</i> pSWEET-COM.	52
Figure 3-4. Growth curves of <i>B. subtilis</i>	53
Figure 3-5. Fluorescence microscopy of <i>B. subtilis</i>	54
Figure 3-6. Gel of extracted RNA from <i>B. subtilis</i> 168 pSWEET-COM.....	55
Figure 3-7. Colony PCR of pSWEET + codon-optimized genes.	56

List of Tables

Table 2-1 MICs in *Streptomyces* liquid media. 27

Table 2-2. MICs of *Streptomyces* on solid media..... 28

Table 2-3. cblaster results in non-*Streptomyces* organisms identifying the presence of the putative resistance cluster from the enugumycin producer..... 35

Table 2-4. MICs of WAC strains..... 43

Table 3-1. MICs in *B. subtilis*..... 50

List of Abbreviations

AMR	Antimicrobial resistance
ARG	Antibiotic resistance gene
BGC	Biosynthetic gene cluster
CWA	Cell wall amidase
CWG	Cell wall glycosidase
CWP	Cell wall peptidase
eDNA	Environmental DNA
FDAA	Fluorescent D-amino acid
GlcNAc	N-acetylglucosamine
GPA	Glycopeptide Antibiotic
HADA	Hydroxycoumarincarboxylamino-D-alanine
HK	Histidine kinase
LB	Lennox broth
mDAP	Meso-diaminopimelic acid
MIC	Minimum inhibitory concentration
MGE	Mobile genetic element
MurNAc	N-Acetylmuramic acid
PBS	Phosphate-buffered saline
PG	Peptidoglycan
RBS	Ribosomal binding site
RR	Response regulator
SAM	<i>Streptomyces</i> Antibiotic Media
TCS	Two-component system
TSBY	Tryptic Soy Broth Yeast
WAC	Wright Actinomycete Collection

Declaration of Academic Achievement

Alexandra Barkhouse performed the majority of experiments, data collection, and analysis presented in this thesis.

Dr. David Sychantha helped in the conception of the topic of this thesis.

Supervisor Dr. Gerry Wright and committee members Dr. Marie Elliot and Dr. Cameron Currie provided guidance and direction throughout the project.

Computational experiments were completed with the help of Dirk Hackenberger.

The Elliot lab donated strains for the conjugation and manipulation of *Streptomyces*.

Chapter 1

1.0 Introduction: The Investigation of Self-Resistance Mechanisms in Environmental Bacteria Can Alleviate the Antibiotic Resistance Crisis

The discovery of antibiotics in the early 20th century saved millions of lives. These compounds continue to cure diseases and alleviate suffering.¹ Despite antibiotics' critical role in our lives, antimicrobial resistance (AMR) curbs their efficacy in treating infection. Resistance to antibiotics can be acquired through the transference of antibiotic resistance genes (ARGs) from resistant to susceptible bacteria. This process is influenced by mobile genetic elements (MGEs), which are often associated with ARGs and can move within or between bacterial chromosomes.^{2,3} It is widely accepted today that environmental bacteria – which house self-resistance mechanisms against their secreted antibiotics – could be the origin of clinical resistance. However, self-resistance is not the only origin of AMR. Resistance is not exclusive to pathogenic bacteria, as seen first by Benveniste and Davies when they discovered that several *Streptomyces* species contained aminoglycoside-inactivating enzymes similar to those seen in clinical isolates; since then, several researchers have reported similar findings.⁴⁻⁶ This trend has been seen in more recent metagenomic screens of clinical resistance genes identified in soil. Thus, the likely source of these resistant bacteria originates from the environmental reservoir of resistance genes or the “environmental resistome.”

The dissemination of ARGs is encouraged by antibiotic over-prescription in the clinic and their exploitation in agriculture and animal production.^{7,8} Ultimately, to combat the ever-evolving selection for AMR in clinically relevant bacteria, discovering novel antibiotics is paramount; however, understanding new resistance mechanisms to these compounds is just as important.

Among the first instances of drug-resistant bacteria was seen in the clinic shortly after the widespread use of the newly discovered penicillin.^{9,10} This pattern has been consistent with the discovery of most new antibiotics. Within a decade of clinical use, resistant pathogenic strains have been identified. An exception is vancomycin resistance, which emerged ~30 years after its introduction to the clinic.^{11,12} The rate at which these microbes select for resistance to combat these bioactive compounds makes the need for new antibiotics acute. However, it is a low priority for the pharmaceutical industry as these compounds are not financially lucrative.

Understanding the self-resistance mechanisms seen in environmental bacteria can aid in more effectively treating bacterial infections. If resistance were to arise against novel antibiotics, an alternative treatment route could be more easily explored based on the knowledge of the environmental self-resistance mechanism. For instance, antibiotic adjuvant compounds can be developed with a complete comprehension of the mechanisms of bacterial resistance.¹³ Another approach could involve manipulating the fitness cost of these resistance mechanisms. Where bacterial strains are resistant to one antibiotic, they could be more susceptible to another antibiotic that would have been previously ineffective.¹⁴ This could be achieved by using the two antibiotics together in combination therapy, where one induces the resistant phenotype, and the other can take advantage of the defects in the cell due to the resistant phenotype's biological fitness cost. Regardless of the strategy used to combat clinical resistance, with the knowledge of environmental resistance mechanisms, there are endless applications in drug development and clinical treatment.

The inspiration behind this thesis was to explore the self-resistance mechanism of murobactin (Type V glycopeptide) antibiotics. Dr. Min Xu first identified a putative resistance cassette within murobactin producers.¹⁵ The first step in investigating this putative resistance mechanism

starts with understanding *Streptomyces* sp., how and why they can produce many antimicrobials, and the peptidoglycan (PG) biosynthesis and remodelling process. Next, suitable hosts must be used to house these hypothetical resistance genes; minimum inhibitory concentration assays (MICs) and phenotypic analyses should then be performed to document any acquired resistance. The experiments in this thesis use many approaches to try and confirm the function of this gene cluster.

1.1 *Streptomyces* – the Reservoir of Novel Antibiotics and Novel Resistance Mechanisms

One notable phylum that has been exploited for its natural product antibiotics is Actinomycetota. These Gram-positive bacteria have genomes with high G+C content and are widely distributed across aquatic and terrestrial domains. One genus of particular interest is *Streptomyces*. Like many other members of the Actinomycetota phylum, *Streptomyces* produce a mycelium and reproduce through sporulation. Their growth pattern involves tip extension and branching hyphae (Fig. 1-1).¹⁶

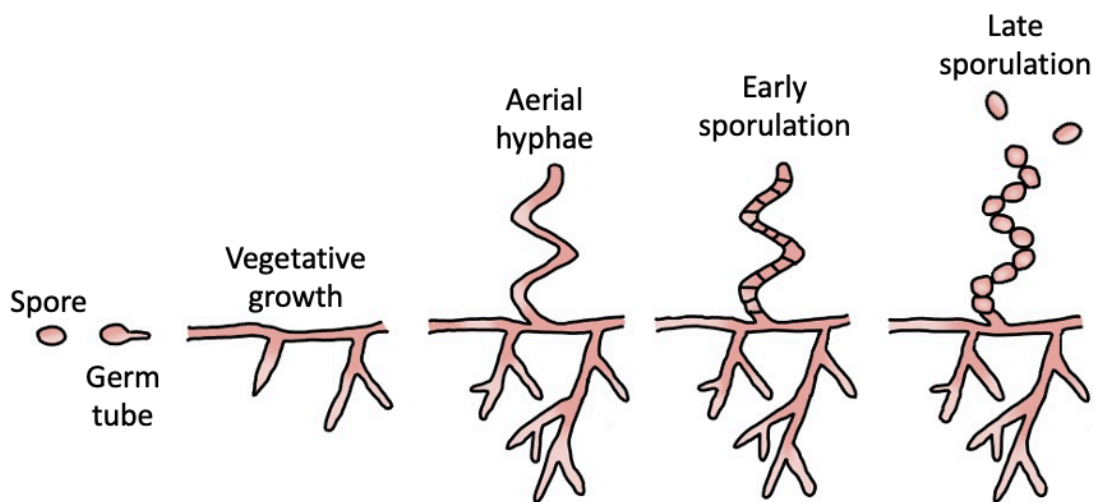


Figure 1-1. Illustrated developmental life cycle of *Streptomyces*. Adapted from Flardh et al., 2009.

These bacteria typically grow in moist environments, and when stressed or exposed to hydrophobic micro-environments, this induces aerial hyphae formation. These organisms incorporate an external hydrophobic rodlet layer to allow bacteria to escape from aqueous environments. A complex of two types of proteins work together to form the rodlet layer; rodlins are proteins which form rod-shaped fibrils, and chaplins are smaller hydrophobic proteins.¹⁷ The purpose of the rodlet layer is to help break the surface tension of the aqueous-air interface. When rodlins are absent, aerial hyphae do not lose their hydrophobicity; this implies that other proteins play a prominent role in surface hydrophobicity, with chaplins being excellent candidates.¹⁸ In a strain lacking all chaplin genes, aerial growth is severely impaired.¹⁷

Chaplins are not the only small hydrophobic peptides involved in raising aerial hyphae. SapB has surfactant properties and can also break surface tension efficiently.^{18,19} SapB was first isolated from surface spores but can also be found in culture media.¹⁸ SapB is often seen on aerial structures.¹⁸ Fungal strains also contain small hydrophobic peptides called hydrophobins. These proteins are secreted as monomers similar to chaplins and aggregate when they encounter surfaces or interfaces.^{20,21} They also share the surfactant properties with SapB and chaplins. Small hydrophobic peptides are commonly found in sporulating organisms and are important to their cellular development and the dispersion of spores into the environment.¹⁸

Streptomyces are abundant in soil, these bacteria contribute significantly to soil ecology and are known for their ability to produce a vast diversity of secondary metabolites.²² As their environment is often crowded with other soil-dwelling microbes, producing compounds that are toxic to these organisms frees up resources for *Streptomyces* in the environment. Secondary metabolites isolated from the Actinomycetota phylum make up two-thirds of natural product antibiotics currently used in the clinic, a large proportion of these bacteria belonging to the

Streptomyces genus.²² Cell wall-acting antibiotics produced by *Streptomyces* species include beta-lactams and glycopeptides, among others.

Bacterial genomes encode numerous proteins and enzymatic mechanisms to ensure the host cell's survival. Many bacteria also encode biosynthetic gene clusters (BGCs), including the genes necessary to produce the antibiotics we see in nature and use in the clinic.²³ BGCs are abundant in *Streptomyces*.²⁴ Generally, a BGC can be defined as two or more grouped genes that encode enzymes of a particular biosynthetic pathway leading to the production of a secondary metabolite. BGCs can also contain genes encoding proteins that function in transport mechanisms, regulatory elements, and other enzymes to modify the created compound.²⁵⁻²⁷ Antibiotic-producing BGCs also often possess a cognate resistance mechanism.²⁸ Investigating these resistance mechanisms and their mode of action can yield a better understanding of the possible mechanism of resistance to be developed through bacterial selective pressure. In previous literature, novel antibiotics have been isolated from *Streptomyces* species using the information encoded within these BGCs in concert with in-depth phylogenetic analyses. For example, the Wright lab has used known self-resistance genes from glycopeptide producers (*vanHAX*) to distinguish producers of “true” glycopeptides from potential novel antibiotics within this family and applied this strategy to identify corbomycin. This antibiotic does not possess *vanHAX*-mediated resistance.²⁹ Thus, understanding the cognate resistance mechanism encoded within a known producer can be leveraged in modern antibiotic discovery.

Due to *Streptomyces*' extensive natural product production potential, these organisms can encode a variety of self-resistance mechanisms to these self-produced compounds. For example, regarding DNA-damaging molecules alone, *Streptomyces* have evolved multiple encoded resistance mechanisms: sequestration, modification, efflux, self-sacrifice, DNA repair protection,

and metabolic dormancy.³⁰ As there can be a wide diversity of resistance mechanisms against a single class of antibiotics, it is a fair conclusion that these bacteria may house numerous resistance mechanisms to several compounds. In the case of chloramphenicol production in *Streptomyces venezuelae*, *cmlV* is a chloramphenicol-specific exporter.³¹ This gene encodes a transmembrane-spanning protein that is present within the chromosome, but not in the corresponding BGC. It is, however, important to note that this form of self-resistance has yet to be seen or transferred to clinical isolates.^{24,31,32} An example of a self-resistance mechanism from *Streptomyces* emerging in the clinic is streptomycin resistance, from *Streptomyces griseus*. StrA-StrB are phosphotransferase enzymes that inactivate streptomycin and have been identified in commensal and pathogenic bacteria of animals, humans, and plants. In this case, disseminating these resistance genes can increase the probability of their uptake into pathogenic bacteria and render infection treatment ineffective.³³ *Streptomyces*, which produce beta-lactam drugs, have also been seen to harbour resistance mechanisms found in clinical isolates.³⁴ These examples further prove a previously mentioned point: resistance can originate from soil microbes.

Antibiotics can target numerous vital biological functions. Generally, antibiotics will inhibit or manipulate five processes in the bacterial cell: PG synthesis, cytoplasmic membrane composition and integrity, translation, transcription, and nucleic acid replication.³⁵ In the context of my research, PG as a drug target is particularly relevant. First, to understand the mechanism of action for antibiotics targeting PG, it is pertinent to understand its composition and synthesis thoroughly.

1.2 Peptidoglycan Biosynthesis & Remodeling & Peptidoglycan as a Drug Target

Two aminosugars comprise the primary subunits of PG: *N*-acetylglucosamine (GlcNAc) and *N*-acetylmuramic acid (MurNAc). These aminosugars are connected by a β -1,4 glycosidic bond,

forming a disaccharide core subunit. MurNac contains a lactyl group, which allows for the attachment of a pentapeptide. The amino acids within this pentapeptide can vary depending on the bacterial species. Still, typically, the pentapeptide begins with L-Ala, which forms an amide bond with the pendant carboxyl of the lactyl group of MurNac, followed by D-Glu in the second position and terminated with D-Ala-D-Ala. The residue in position 3 varies between species but is often a basic amino acid such as Lys or meso-diaminopimelic acid (mDAP). The terminating dipeptide D-Ala-D-Ala can also vary, although this is less frequent.³⁶ Crosslinked isopeptide bridges connect the pentapeptides through a transpeptidation reaction catalyzed by transpeptidases, also known as penicillin-binding proteins (PBPs). This event occurs at position 4 D-Ala on one peptide and the dibasic position 3 residue on the other (Figure 1-2). The PG structure can be further modified by carboxypeptidases, endopeptidases, and several other autolysins for cell wall remodelling, cell division, or biosynthesis.³⁷

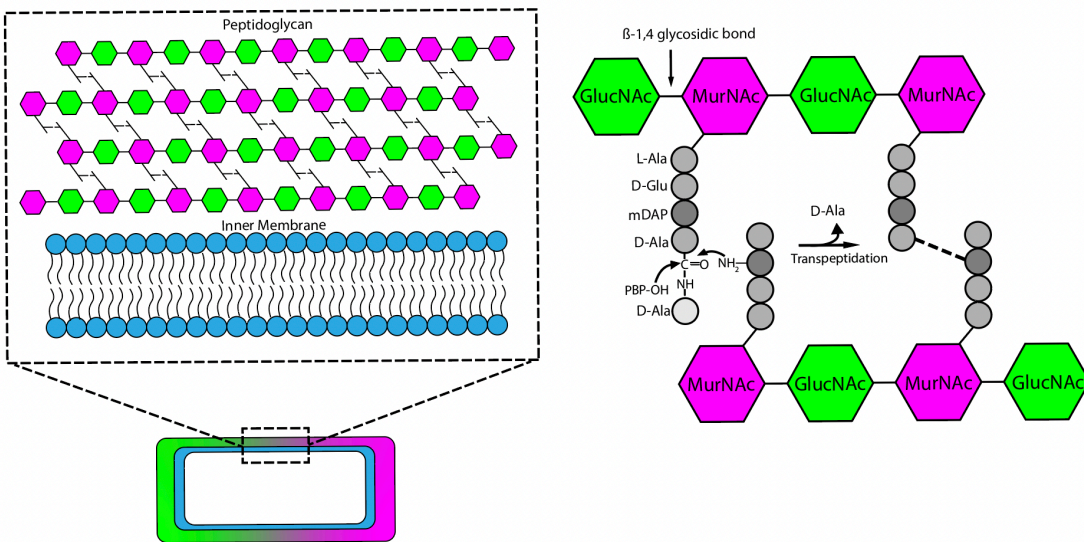


Figure 1-2. Simplified scheme of PG biosynthesis. Pink and green represent the two aminosugars that comprise PG. To the right is a closer look into the enzymatic reaction that forms the crosslinks found in *N*-acetylmuramic acid. This schematic is explicitly referencing a Gram-positive bacterium.

PG biosynthesis starts with forming nucleotide-activated sugars and amino acids in the cytoplasm. This process begins with UDP-GlcNAc, which is converted to UDP-MurNAc by the enzymes MurA and MurB. The stem peptide is added to the lactyl moiety of MurNAc, starting with L-Ala catalyzed by the enzyme MurC. The second residue in the pentapeptide, D-Glu, is added by the enzyme MurD following the racemization of L-Glu by MurI. The third residue is variable, as previously mentioned; commonly, this can be mDAP or L-Lys, the addition of which is catalyzed by MurE. The D-Ala-D-Ala dimer is synthesized by D-Ala-D-Ala ligase and added to the stem peptide by MurF.

Lipid I comprises the inner membrane lipid carrier, undecaprenyl pyrophosphate (UndPP) – embedded in the bacterial cytoplasmic membrane – and UDP-MurNAc. The enzyme MraY catalyzes the transfer of UDP-MurNAc-pentapeptide to UndPP which is embedded in the bacterial cytoplasmic membrane generating lipid I. The addition of GlcNAc to lipid I is catalyzed by the enzyme MurG, resulting in the formation of Lipid II. Lipid II comprises the disaccharide GlcNAc-MurNAc (with the attached stem peptide) and UndPP.³⁸ Lipid II is then translocated to the outer leaflet of the cytoplasmic membrane by several flippases. Once positioned outside the cell, transglycosylases, many of which are bifunctional transglycosylase-PBPs, catalyze the addition of this new PG subunit to the growing cell wall.³⁸ Eventually, the lipid anchor and the accompanying pyrophosphate are reused and shuttled back to the cytoplasmic membrane for subsequent PG biosynthesis.

To allow for the expansion of PG during cell elongation, the covalently closed mesh that is formed after its biosynthesis must be opened. PG expansion involves the controlled cleavage of the glycan portion of the cell wall by hydrolases to make space for new PG strands.³⁹⁻⁴¹ Bacteria encode several PG hydrolases. Vermassen et al.⁴² have grouped these cell wall hydrolases into

three general categories: cell wall amidases (CWA), cell wall glycosidases (CWG), and cell wall peptidases (CWP). CWAs cleave the bond between MurNAc and L-Ala at the N-terminal of the pentapeptide. A well-known CWA is AmiA, found in *E. coli*.⁴³ CWGs catalyze the hydrolysis of glycosidic linkages between the aminosugars GlcNAc and MurNAc; in the context of PG remodelling, this refers to the bond between the two aminosugars, GlcNAc and MurNAc. Here, CWGs can be further differentiated into *N*-acetylglucosamidases and lysozymes.⁴⁴ CWPs cleave the amide bond between amino acids. These hydrolases can be distinguished by their endopeptidase or carboxypeptidase activity; respectively, they cleave within the pentapeptide or remove C-terminal amino acids.⁴⁵ A schematic illustrating the cleavage sites of each type of cell wall hydrolase can be found in the review paper by Vermassen et al.⁴²

PG and its assembly are desirable drug targets as humans do not have an equivalent to this vital bacterial structure. While the PG wall is thicker in Gram-positive bacteria at 30-100 nanometers, the layer is thinner at only a few nanometers in Gram-negative bacteria and guarded by the outer membrane. Antibiotics can target several processes within PG biosynthesis.⁴⁶ Fosfomycin is a natural product in the phosphonic acid class of antibiotics, isolated from *Streptomyces* sp., that targets MurA; where MurA enzyme catalyzes the first steps of PG biosynthesis, allowing the transfer of enolpyruvate from phosphoenolpyruvate (PEP).⁴⁷ Bacitracin is another natural product in the cyclic peptide class of antibiotics isolated from multiple *Bacillus* sp., which binds undecaprenyl pyrophosphate and prevents its recycling to a monophosphate form.⁴⁸ The beta-lactam antibiotics, including penicillins, cephalosporins, and carbapenems, inhibit the PBP transpeptidases. Among the first of their kind, meroquinolones antibiotics have been shown to inhibit autolysin activity, affecting PG remodelling.²⁹

1.3 Glycopeptide Antibiotics & Resistance

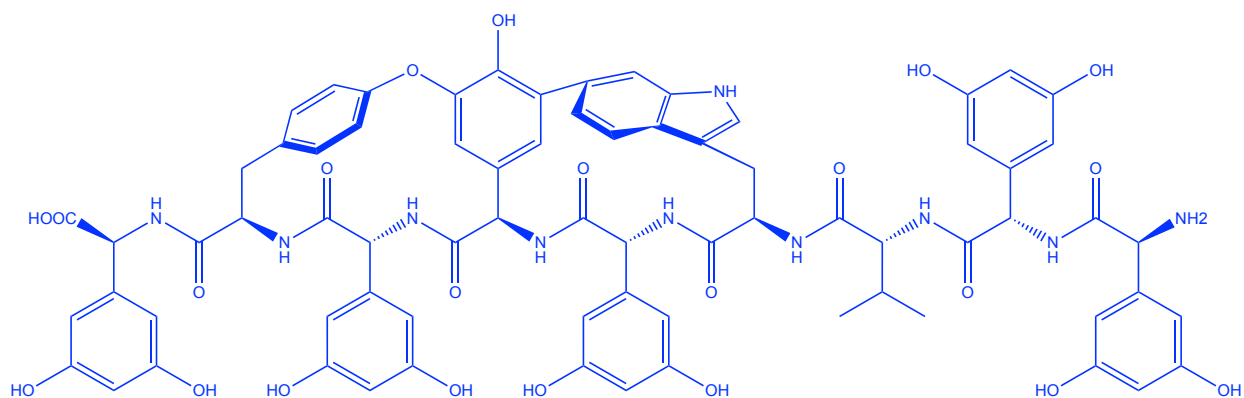
Glycopeptide antibiotics (GPAs) bind to the acyl-D-alanyl-D-alanine (D-Ala-D-Ala) terminus of the growing PG chain in Gram-positive bacteria to prevent biosynthesis and cross-linking. The mechanism specifically targets lipid II and immature PG, leading to a lack of cell wall rigidity that induces cell lysis and is thus bactericidal.⁴⁹ Vancomycin was discovered in 1957, isolated from *Streptomyces orientalis* found in a remote region of Borneo. This antibiotic is utilized as a first-line agent for infections caused by methicillin-resistant staphylococci and finds use in treating infections caused by many other Gram-positive pathogens.⁵⁰

Vancomycin resistance is achieved by replacing the D-Ala-D-Ala terminus with D-alanyl-D-lactate (D-Ala-D-Lac) or D-alanyl-D-serine (D-Ala-D-Ser), with the substitutions reducing the antibiotic target affinity by 1000-fold and 7-fold, respectively.⁵¹⁻⁵³ The *vanHAX* core of genes is responsible for resistance to GPAs in pathogens, and homologues of these genes have been identified in most published glycopeptide-producing strains.^{46,54} Typically, these resistance genes are found in the biosynthetic gene cluster; however, this is not always the case. VanH produces D-Lac precursors through its action as a D-Lac dehydrogenase. VanA is a ligase specific for D-Ala-D-Lac, catalyzing the formation of the depsipeptide. VanX is an enzyme that recognizes and cleaves the D-Ala-D-Ala terminus but does not cleave the modified D-Ala-D-Lac.^{46,54} VanG is a structurally similar ligase to VanA but has higher selectivity towards D-Ser over D-Lac.⁵⁵ The *vanHAX* core is controlled by a two-component regulatory system (TCS) VanRS. This system comprises the sensor histidine kinase VanS and VanR, a response regulator. VanS can recognize the complex of vancomycin (or other GPAs) bound to the pentapeptide of PG.⁵⁶ VanS sends this

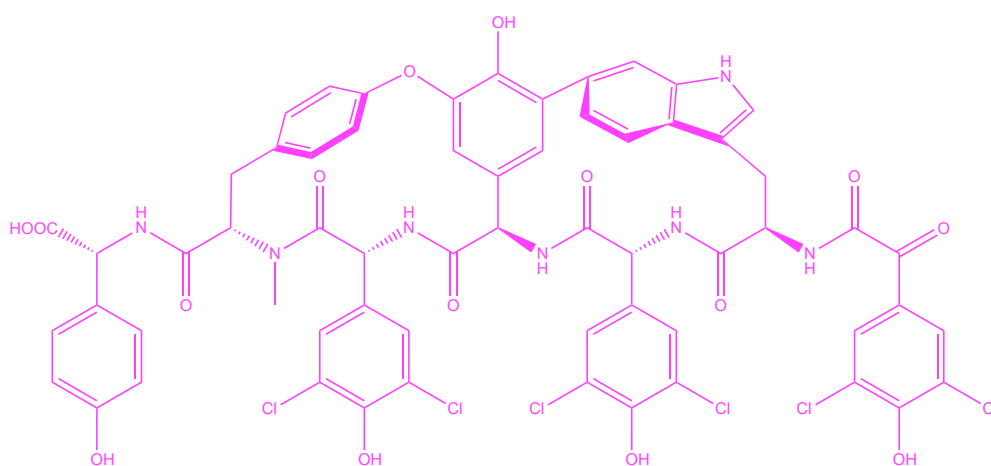
signal through autophosphorylation and subsequent phosphorylation of the Asp residue on VanR. The phosphorylated VanR binds upstream of the *vanHAX* cluster, inducing gene transcription.⁵⁷

Vancomycin is only one of five subtypes of GPAs; these antibiotics are classified based on their amino acid content and cross-linking pattern.⁵⁸ Generally, Type I-IV GPAs bind D-Ala-D-Ala and are formed from a heptapeptide scaffold. The mechanism of action for all these subclasses of antibiotics is the same. Recently, the Wright Lab discovered multiple Type V GPAs, which we term murobactins.^{29,59} In the context of this thesis, the nonapeptide, enugumycin and the previously reported heptapeptide, complestatin (Figure 1-3), are particularly relevant as I focused on their bioactivity and resistance.

Murobactins contain a defining tryptophan residue and a C-C linkage between this residue and the central amino acid 4-hydroxyphenylglycine (Hpg).^{15,58} Some murobactins contain a nonapeptide scaffold, but many incorporate a heptapeptide backbone. The mechanism of action for these compounds differs from the typical D-Ala-D-Ala-binding glycopeptides. Instead, unpublished work in the Wright lab shows that murobactins primarily bind the sugar components of PG, leading us to propose an alternative nomenclature for these compounds.



Enugumycin



Complestatin

Figure 1-3. Chemical structure of enugumycin & complestatin. Both muobactins possess a tryptophan (Trp) linked to a central 4-hydroxyphenylglycine (Hpg). Notably enugumycin has a rare nonapeptide scaffold.

1.4 Murobactin Antibiotics & Resistance

The mechanism of action for murobactin antibiotics makes these compounds unique. By binding directly to the glycan portion of PG, these compounds prevent autolysin activity and interfere with proper cell division. In contrast to D-Ala-D-Ala-binding glycopeptides that inhibit PG biosynthesis, this action by murobactins results in a bacteriostatic phenotype.²⁹ In all studied subclasses of glycopeptides, a resistance mechanism, like the *vanHAX*, is co-located in the BGC. In contrast, murobactin-producing bacteria do not contain the characteristic *vanHAX* cluster homologues.¹⁵ Thus, the self-resistance mechanism for murobactin antibiotics remains elusive, and the work described in this thesis aimed to uncover the strategy by which producing bacteria avoid self-intoxication. Several murobactin-producing bacterial strains have been shown to contain four to six conserved genes within their BGCs that were hypothesized to contribute to self-resistance (Fig.1-4).

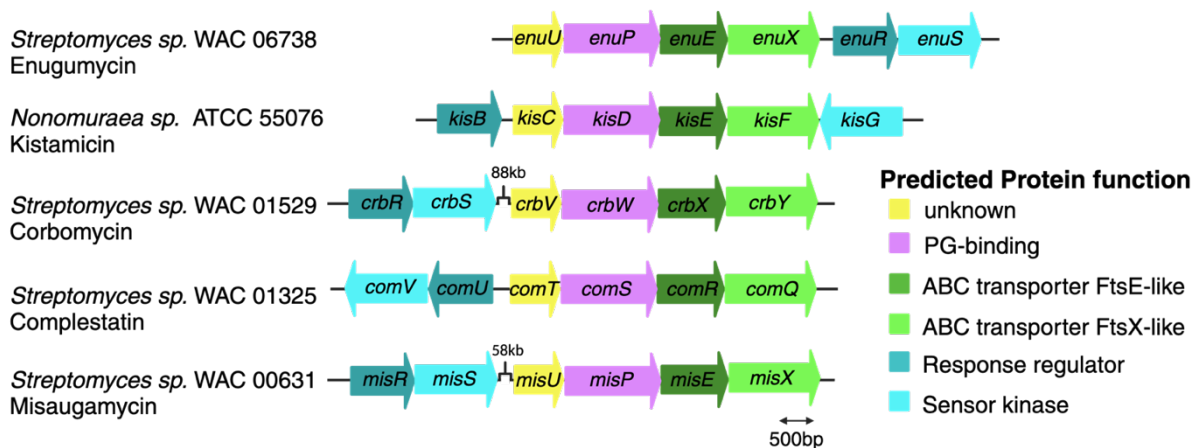


Figure 1-4. Conserved putative resistance cassette for murobactin antibiotics within producer strain BGCs. The hypothetical resistance core comprises FtsEX-like proteins, a protein with a PG-binding domain, and one protein with an unknown function. The cassette is potentially regulated by a TCS homologous to *vanRS*. TCS genes are separated by 88,441 bp and 58,053 bp in WAC 01529 and WAC 00631 BGCs, respectively.

This thesis aimed to investigate the putative resistance mechanism of murobactin antibiotics, specifically from *Streptomyces sp.* WAC06738 and *Streptomyces sp.* WAC01325. The putative

resistance cassettes encode *enuS/comV* and *enuR/comU*, which were identified by homology to the proteins comprising the TCS for vancomycin resistance (VanRS). The remaining gene cassette consists of *enuU/comT*, *enuP/comS*, *enuE/comR*, and *enuX/comQ*, whose biochemical functions are unknown. The genes *enuE/comR* and *enuX/comQ* are predicted to encode proteins homologous to FtsX and FtsE proteins, respectively. FtsEX belongs to the ATP binding cassette (ABC) transporter family.⁶⁰ EnuP/ComS possesses a putative cell wall binding domain tethered to an adaptor domain.⁶¹ This adaptor domain is known to interact with ABC-transporters in other contexts.⁶² Therefore, I hypothesized that the mechanism of resistance involves the EnuRS/ComUV-regulated action of EnuUPEX/ComTSRQ, which may act in concert to displace murebactin bound to the cell wall (Figure 1-5).

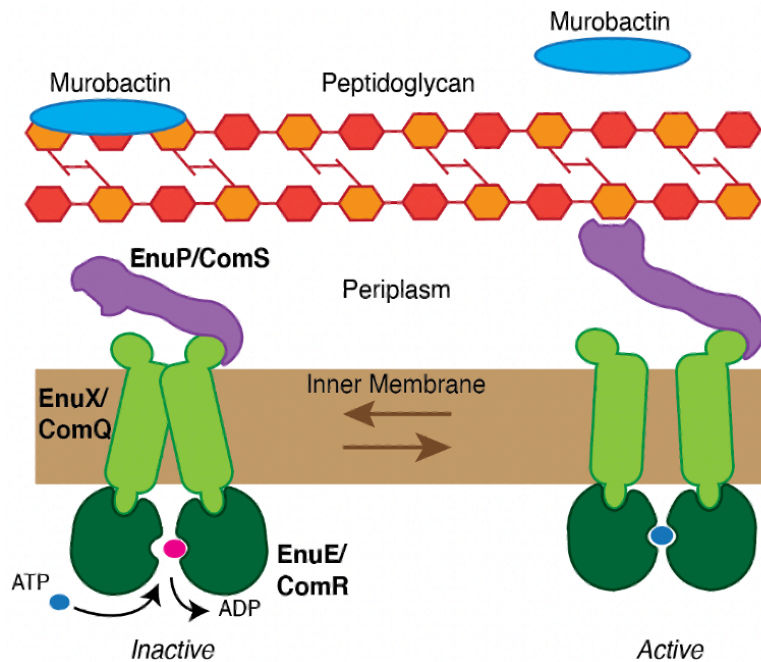


Figure 1-5. The potential mechanism of action for the putative resistance protein complex. The hydrolysis of ATP by the ATPase (EnuE/ComR) components causes a conformational change, sending a mechanical signal to the PG-binding protein (EnuP/ComS), allowing it to bind to PG. This could be initiated by the murebactin binding to the PG or the corresponding TCS system.

When bacteria produce an antibiotic, they encode a cognate resistance cassette for host cell survival. These resistance genes can be regulated by a TCS such as VanRS. When confronted with a sudden environmental change, TCSs are essential in maintaining homeostasis within bacterial colonies. TCSs initiate a response to a chemical or physical signal. In the context of antibiotic resistance, the induction of this signal can be caused by bound antibiotics or the resulting biochemical impact caused by these compounds. However, the stimuli that induce TCSs can be ambiguous.⁶³

TCSs comprise two proteins: a sensor histidine kinase (HK) and a response regulator (RR). Generally, HKs consist of two domains: a variable N-terminal input domain located within the extracellular or periplasmic space and a conserved C-terminal domain within the cytosol, which interacts with the RR.⁶⁴ The domains of the HK are connected by transmembrane helices, the number of which is dependent on the system. The RR is a homodimeric protein located in the cytosol and consists of the N-terminal conserved receiver domain and the variable C-terminal output domain. The N-terminus of the HK senses conformational changes, environmental changes, or the direct binding of a ligand. This structural rearrangement induces autophosphorylation through ATP-hydrolysis on a histidine residue within its conserved C-terminus.⁶⁵ The phosphate bound to the histidine is then transferred from the HK C-terminus to an aspartate residue within the conserved N-terminus of the RR. Phosphate binding activates the variable C-terminus of the RR, inducing DNA targeting to regulate gene transcription.⁶⁵ In this way, bacteria can readily adapt to environmental changes and transmit information from the external environment to the cell interior through the induction of gene transcription.

Within the BGC for vancomycin, the VanRS-regulated resistance gene cassette is used, as previously mentioned. ⁶⁶ Wright et al.⁶⁷ concluded that using a fusion protein consisting of

maltose binding protein (MBP) and the cytoplasmic domain of VanS derived from vancomycin-resistant enterococci, this HK catalyzes both the autophosphorylation of itself as well as the transference of its bound phosphate to VanR.⁶⁷ Holman et al.⁶⁸ then identified that phosphorylated VanR (P-VanR) strongly bound the promoter for *vanH*, which induces the transcription of the *vanHAX* operon.⁶⁸

As countless antibiotics are produced from bacterial species, equally diverse antibiotic resistance mechanisms are utilized for survival. Namely, the main resistance mechanisms involve limiting drug uptake, modifying the drug target, enzyme-inactivation of the drug, or drug efflux from the bacterial cell.⁶⁹ ATP-binding cassette (ABC) transporters are often involved in the efflux of antibiotics from the cell interior. These complexes make up one of the largest membrane protein families in prokaryotes. ABC transporters consist of two widely conserved cytoplasmic subunits that bind nucleotides and two transmembrane subunits; typically, the latter will form a membrane component of the complex.⁷⁰ ABC transporters, not limited to the context of antibiotic resistance, can import or export substrates. Interestingly, these complexes can mechanically transmit signals across the cell membrane using the energy provided by ATP hydrolysis. One defined member of the ABC transporter superfamily is FtsEX. In this case, FtsX is a membrane component protein, and FtsE is an ATPase responsible for transmitting a conformational signal from the cytosol to the periplasm; therefore, FtsEX is not, by definition, a transporter. This complex is crucial to bacterial cell division, as it actively recruits cell wall hydrolases to allow septal division and create new daughter cells.⁶⁰

One example of intrinsic resistance that employs interfacing between a TCS as well as an ABC transporter is the BceAB-RS detoxification system found in *Bacillus subtilis* that prevents the antibiotic bacitracin from binding to the lipid II intermediate UndPP in PG biosynthesis.⁷¹

The ABC transporter complex constitutes BceA, which has two ATPase domains and BceB, which is a transmembrane permease. The TCS comprises the HK BceS, that phosphorylates the RR BceR. Notably, BceS lacks an extracellular ligand-binding domain. BceAB has been shown to promote resistance by freeing UndPP from bacitracin following complex formation; the mechanism by which this occurs is unknown.⁷¹ However, Dintner et al.⁷² demonstrated that through bacterial two-hybrid assay and *in vitro* pull-down assays, the BceAB transporter complexes with BceS HK.⁷² Initially, it was thought that the BceAB-RS system was a typical drug efflux resistance mechanism. However, there was no evidence to support this claim. Soon after, BceAB was hypothesized to import bacitracin into the cell and subsequently degrade the drug. However, the most widely accepted theory is that BceRS-AB provides target protection of cell wall synthesis by releasing lipid II intermediates UndPP from bacitracin binding.⁷³

1.5 Project Objectives

To better prepare for the emergence of AMR to novel antibiotic compounds, it is critical to understand the self-resistance mechanisms found in antibiotic producers in case this resistance is seen in the clinic. The work described in this thesis took many approaches to identify the resistance mechanism of murebactin antibiotics in two model organisms. The first chapter of this thesis highlights those methods used in *Streptomyces venezuelae*, and the second chapter highlights experiments done in *B. subtilis*. The two different model organisms were used to elucidate different information. As *S. venezuelae* is a well-characterized species from the *Streptomyces* genus and is susceptible to the effects of murebactins, introducing resistance genes into its genome would be expected to confer resistance. Since the genus is naturally G+C rich, there should be no problem expressing the putative resistance proteins down the line, as they are from an equivalently G+C rich producer strain. *B. subtilis* is one of the best-known Gram-

positive model organisms and has also been seen to have an elongated phenotype when exposed to murobactins.²⁹ Thus, if a healthy cell phenotype is returned upon introducing a putative resistance cassette into *B. subtilis*, this would be evidence of the gene cassette conferring resistance to murobactin antibiotics. If investigating this gene cassette is not fruitful, an alternative method to uncover this resistance mechanism would be to use the *FatI* partial digestion method for metagenomic library preparation.⁷⁴ The goal of this thesis is to investigate the self-resistance mechanism of murobactin-producing bacterial strains.

Chapter 2: Assessing a putative resistance mechanism using *Streptomyces* as a host

2.1 Introduction

While *Streptomyces* species often house resistance genes for many antibiotics, not all *Streptomyces* are resistant to the compounds other species produce. As *Streptomyces* is a Gram-positive genus, they are a possible target of meroactin antibiotics. When tested, *S. venezuelae* and *Streptomyces coelicolor* were susceptible to complestatin.²⁹ Antibiotic susceptibility was confirmed in this thesis with MICs of wild-type *S. venezuelae* and *S. coelicolor* to both complestatin and enugumycin.

As this research aimed to understand the function of the putative resistance gene cluster, it was important to identify a susceptible host of similar genetic background. The first step in this project was to create strains of susceptible organisms containing the putative resistance genes, expose these strains to meroactins, and record any changes in antibiotic activity by measuring MICs. As both complestatin and enugumycin were extracted from WAC strains of the *Streptomyces* genus, we predicted that the putative resistance genes from both producers were likely to be properly expressed upon their integration into the *S. venezuelae* and *S. coelicolor* chromosomes. These strains can later be used for further investigation into the function of this gene cluster.

2.2 Materials & Methods

2.2.1 Constructs Made with pIJ10257

The plasmid pIJ10257 was donated by Dr. Divya Panchel and transformed into *Escherichia coli* TOP10 chemically competent cells. Plasmid DNA was then isolated using the GeneJET Plasmid Miniprep Kit following the accompanying protocol. This plasmid was then digested using the restriction enzymes *Hind*III and *Nde*I, and was treated with phosphatase before using the GeneJET Gel Extraction kit and protocol for DNA cleanup. Restriction cloning

primers were developed using Geneious Prime software to select the best primer pair, restriction sites, and sufficient overhang on the 5' end of primers for efficient digestion. Two plasmids containing the BGCs of enugumycin and complestatin constructed by Dr. Min Xu were used as template DNA in these PCR reactions. The amplicons of interest consisted of the putative resistance cassette (pIJ10257-EnC) – which consists of all six genes including the putative TCS – and the putative resistance core – the four genes not including the putative TCS – for enugumycin (pIJ10257-Enu) and complestatin (pIJ10257-COM). Reaction products were run on a 1% agarose gel to ensure the amplicon was the expected size of the insert. The resulting product was purified using the GeneJET Gel Extraction kit and protocol.

Ligation of the pIJ10257 plasmid with the PCR product was performed using T4 ligase with insert in a 3-fold molar excess of the plasmid following digestion of PCR product. Following ligation, the plasmid was transformed into *E. coli* TOP10 chemically competent cells and plated onto Lennox Broth (LB) plates supplemented with 150 µg/mL of the selection marker hygromycin. Colonies were screened through digestion of the plasmid with *Hind*III and *Nde*I, followed by visualization on a 1% agarose gel. Positive colonies were sent to Plasmidsaurus for plasmid sequencing.

2.2.2 Conjugation of Plasmids into *S. venezuelae* and *S. coelicolor*

Plasmids containing the putative resistance cassette (pIJ10257-EnC) and the putative resistance core for enugumycin (pIJ10257-Enu) and complestatin (pIJ10257-COM) were transformed into the electrocompetent *E. coli* ET12567 with the accompanying helper plasmid pUZ8002. Transformants were screened on plates containing chloramphenicol (10 µg/mL), ampicillin (50 µg/mL), and hygromycin (50 µg/mL). Transformants were then grown in LB broth with antibiotic selection. Conjugation into *S. coelicolor* was performed following the protocol described in Practical Streptomyces Genetics.⁷⁵ Conjugation into *S. venezuelae* used

overnight cultures directly, and the antibiotic selection overlay containing nalidixic acid (25 µg/mL) and hygromycin (50 µg/mL) was performed ~12 hours after original plating as soon as pigment was visible on soy flour mannitol agar (SFM) plates containing 10 mM MgCl₂ (Appendix 1). Exconjugants were streaked onto SFM plates with hygromycin (50 µg/mL) for further selection.

2.2.3 MICs of Murobactins in *Streptomyces* and Wright Actinomycetes Collection Strains

Overnight cultures were made in 3 mL of Tryptic Soy Broth Yeast (TSBY) (Appendix 1) with three glass beads (5 mm), with hygromycin (50 µg/mL), for *S. coelicolor* and *S. venezuelae* and all exconjugants. Overnight cultures of WAC strains were grown in *Streptomyces* Antibiotic Media (SAM) media for 5-7 days (Appendix 1). Measurements of the OD₆₀₀ were taken from the overnight cultures and were then diluted to OD₆₀₀ ~0.1 in saline, then diluted to 1:200 in TSBY or SAM. Stocks of antibiotics were made in DMSO. This was done by starting with a concentration of 3.2 mg/mL, then doing two-fold dilutions, 64 µg/mL – 0.0625 µg/mL. Antibiotic stocks (8 µL) were added to 192 µL of TSBY or SAM; this gave a final DMSO concentration of 2%. An equal volume (50 µL) of antibiotic mixture and cells were introduced into a fresh 96-well plate. All MICs experiments were done in duplicate. *Streptomyces* species were incubated at 30°C for 2 days, but WAC strains were incubated for one week. After incubation, a multichannel pipette was used to spot 5 µL saturated antibiotic-treated cells to square plates of Bennet's Agar (Appendix 1), and these were incubated at 30°C for 2 days. MICs were assessed by using a plate reader to approximate OD₆₀₀ measurements.

2.2.4 Assessment of Phenotypic Changes Induced by Murobactin Antibiotics

Samples were collected from MIC plates for analysis by light microscopy. One layer of tape was wrapped around the ends of a microscope slide, this was repeated to have two

microscope slides with tape on each end. A fresh microscope slide was flanked with the taped slides. A mixture of 1.5% agarose and LB media was microwaved until bubbling, then aliquoted into Eppendorf tubes (~800 μ L). The LB agarose was pipetted (80 μ L) onto the middle of the slide, and another slide was placed perpendicularly on top of the agarose. After ~1 minute, the top slide was removed, exposing the agarose. The sample (8 μ L) was spotted onto the agarose by capillary action. A coverslip was placed on the sample and visualized by light microscopy with the EVOS XL core microscope or the Nikon Ci-L+.

2.2.5 *S. venezuelae* and *S. coelicolor* Growth Curves

Plates (96-well) were prepared with 1:400 dilution of overnight cultures from *S. venezuelae* and *S. coelicolor* in TSBY medium, following the same protocol as performed with MICs. Measurements of the OD₆₀₀ were taken every 10 minutes over 48 hours, incubated at 30°C, and shaken at 300 rpm at every measurement point. A larger scale growth curve was also done for *S. venezuelae* by inoculating 100 mL of TSBY with a 1:50 dilution of overnight culture. Dilutions (1:4) of growing culture were made in cuvettes every hour, and OD₆₀₀ measurements were taken in a spectrophotometer until growth no longer increased exponentially. This was considered the ‘manual growth curve’. Data for both methods were visualized using GraphPad software.

2.2.6 Assessment of Peptidoglycan Biosynthesis

Fresh medium (TSBY) was inoculated with an overnight culture of *S. venezuelae* to a dilution of 1:50. Measurements of the OD₆₀₀ were taken until strains were in the log phase of growth. Cells were diluted to OD₆₀₀ ~0.2 in 300 μ L of fresh growth medium. Subsequent steps were performed in opaque Eppendorf tubes. The fluorescent D-amino acid (FDAA) 7-hydroxycoumarincarboxylamino-D-alanine (HADA) was added to a final concentration of 500 μ M, and tubes were left to incubate at room temperature for 45 minutes. Cells were washed with 1mL 1 \times phosphate-buffered saline (PBS) three times. The cell pellet was resuspended in 80 μ L

of $1 \times$ PBS. Fluorescence microscopy was performed, and visualization was achieved using a DAPI laser with an excitation peak at 350 nm and an emission peak at 465 nm. Agarose pads of samples were prepared for microscopy using the method described in section 2.2.4.

2.2.7 Computational Analysis of Putative Resistance Genes

Dirk Hackenberger aided in the computational analysis of these genes of interest using cblaster and AlphaFold. Potential homologues of the putative resistance genes were screened using the tool cblaster; this helps identify co-located hits in BLAST searches against genomic databases. We investigated the NCBI and our custom database of the WAC library. Only organisms that expressed all six genes together were considered to have a high score. The amino acid sequences of the enugumycin producer putative resistance core were compiled into the AlphaFold 2.0 software⁶¹, which predicted the most likely tertiary structure of the individual proteins along with the quaternary structure of the proposed complex.

The genomic context surrounding the putative resistance genes was also explored using cblaster (<https://cblaster.readthedocs.io/en/latest/guide/index.html>) to find examples of the cluster in a database of Actinomycetota genomes (n = 7774 from NCBI). For analysis, only examples that contained all the reference proteins were included. If available, the genetic context was analyzed from 10kb on either side of the ‘resistance’ cassette. If not, we included the available sequence until the end of the contig.

2.2.8 RNA Isolation in *S. venezuelae* and *S. coelicolor* & cDNA Synthesis

Fresh TSBY medium (100 mL) was inoculated with 1:50 dilution of overnight culture from *S. venezuelae* and *S. coelicolor*. Cells were harvested after 8 hours via centrifugation at 4000 rpm for 10 minutes at 4°C and were collected in 15 mL Falcon tubes; the supernatant was removed. Cells were flash-frozen in liquid nitrogen until needed. Cells were resuspended with 1M Tris-HCl (pH 7.5), and lysozyme was added to a final concentration of 10 mg/mL in a total

volume of 300 μ L. The mixture was incubated at 30°C for 9 minutes (*S. venezuelae*). Following incubation, 10-12 glass beads (5 mm) and 4 mL of Trizol were added to the sample tubes; the ratio of cells to Trizol was 1:5. The mixture was vigorously vortexed, then 800 μ L of chloroform was added. Each sample was vortexed to homogeneity and then centrifuged at 4°C for 10 mins at 4000 rpm. The upper aqueous phase was removed and added to a fresh tube. An equal amount of acid phenol-chloroform was added to remove residual protein and RNases. The mixture was vortexed for 30 seconds and centrifuged at 4°C for 10 mins at 4000 rpm. The upper aqueous phase was removed and added to a fresh tube. An equal amount of 100% ethanol was added to the mixture and vortexed. Samples were loaded onto the Invitrogen PureLink RNA mini kit following the manufacturer's directions, and starting at the wash steps. Samples were eluted in 50 μ L nuclease-free water. RNA purity was assessed by electrophoresis on an 1.5% agarose gel. Samples were stored at -80°C or proceeded immediately to cDNA synthesis. RNA was treated with dsDNase for 30 minutes and incubated at 37°C before cDNA synthesis. cDNA synthesis was performed according to the Maxima™ H Minus cDNA Synthesis Master Mix protocol.⁷⁶

2.2.9 RT-qPCR in *Streptomyces*

Reverse Transcriptase quantitative PCR was performed with SYBR Select Master Mix CFX (Applied Sciences) on a Bio-Rad C1000 thermocycler. All primer concentrations were 1 mM, and 2 μ L of cDNA was used as the reaction template. Thermocycling conditions were as follows: 2 minutes at 50 °C, 2 minutes at 95 °C, then 40 cycles of 95 °C for 15 seconds and 59.5°C, 59.1°C or 58.5°C for 1 minute. Quantitative PCR was performed on a Bio-Rad C1000 Thermocycler. Gene-specific primers were used in the RT-qPCR reaction to assess gene transcription in the bacterial cell, the primers are as follows: *enuR FP/RP*, *enuS FP/RP*, *enuU FP/RP*, *enuP FP/RP*, *enuE FP/RP*, *enuX FP/RP*, *comT FP/RP*, *comS FP/RP*, *comR FP/RP*,

comQ FP/RP (Appendix 2). Expression is reported as a fold change using a housekeeping gene (*hrdB*) as a reference (Appendix 2).

2.2.10 Sporulation Assay

Spore stocks of each exconjugant were made according to the protocol from Practical *Streptomyces* Genetics.⁷⁵ A lawn was streaked onto minimal media for *Streptomyces* species (ISP4) and rich media for *S. venezuelae* (MYM). Using a P1000 pipette tip, holes were made in the agar plates to allow for the injection of the antibiotic into the plate. Complestatin (3 µL) was placed in these slots, with concentrations ranging from 8 µg/mL to 2048 µg/mL. Plates were incubated at 30°C for 7 days until sporulation could occur.

2.2.11 Metagenomic Library Preparation of eDNA with *FatI* Partial Digestion

eDNA was isolated from seven soil samples from the United States, Nigeria, France, and four locations in Canada (Manitoba, Holman Island, Nova Scotia, and Hamilton, Ontario) using the DNeasy PowerSoil Pro Kit (Qiagen). eDNA was assessed for fragmentation through gel electrophoresis. eDNA was digested with *FatI* until a visible “smear” was found on an agarose gel. A few different methods were used for purification and size exclusion. Identifying the best method is still in progress. Partial digestion mixtures were extracted with a GeneJet Gel Extraction kit (Thermo Fisher Scientific), Kapa Pure Beads (Roche), and a glass wool column.

2.3 Results & Discussion

2.3.1 pIJ10257 Constructs

Plasmid DNA from clones that grew on hygromycin plates was isolated, and constructs were digested using diagnostic restriction enzymes. Constructs harbouring the expected insert displayed a dropout band on the agarose gel, either ~4kb, for pIJ-Enu and pIJ-COM, or ~3kb for pIJ-EnC. The strain considered COM2 did not exhibit this drop-out band and was not chosen for sequencing and subsequent experiments (Figure 2-1). There was evidence of the expected

dropout bands, and two positive clones from each construct were sent for sequencing, and no mutations were identified within the cloned genes.

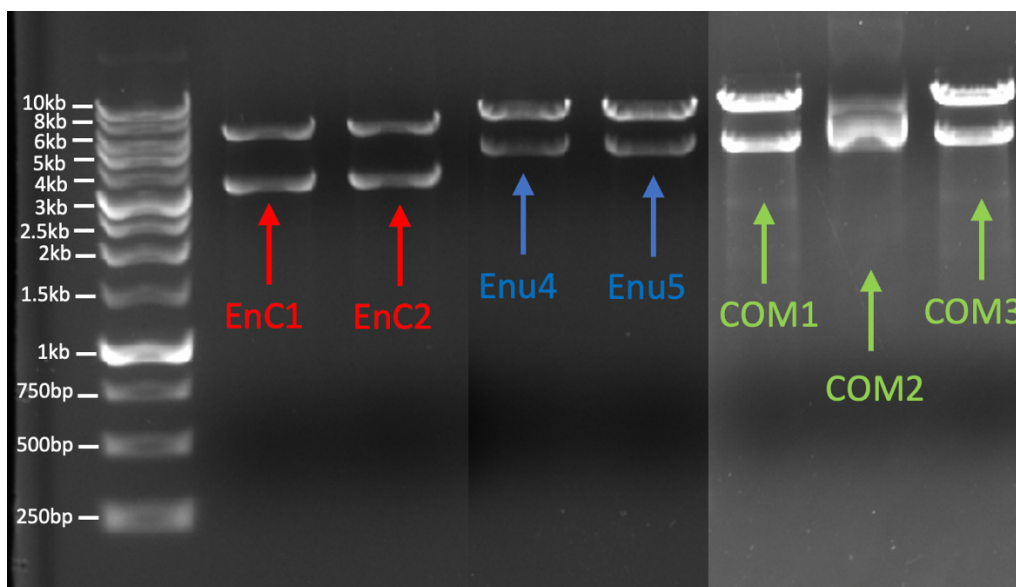


Figure 2-1. Isolated plasmid from positive clones for pIJ10257 constructs containing genes of interest. pIJ-Enu (Enu4, Enu5) and pIJ-COM (COM1, COM2, COM3) were digested by *Nde*I and *Hind*III, yielding dropout bands of ~4kb. pIJ-EnC (EnC1, EnC2) was digested by *Nde*I, *Hind*III, and *Pvu*II, yielding ~3kb dropout band.

2.3.2 MICs of Murobactins in *Streptomyces*

Liquid MICs were performed for *S. venezuelae* ATCC 10712 and *S. coelicolor* M1154 (Table 2-1). MICs for *S. venezuelae* exconjugants against complestatin and enugumycin were not significantly increased or decreased compared to empty vector and wild-type controls (Table 2-1). A similar trend was seen with *S. coelicolor*, save for pIJ-EnC, which does exhibit an increased MIC from both murobactin antibiotics. However, this was only seen in one of two duplicates, while the other duplicate had MICs matching the other two exconjugant strains.

Table 2-1 MICs in *Streptomyces* liquid media. Liquid MICs were performed in TSBY medium in duplicate for both *Streptomyces* species. This table displays the results of liquid MICs. The number refers to the concentration of the merolectin antibiotic in µg/mL at which cells did not grow.

	Complestatin (µg/mL)	Enugumycin (µg/mL)
<i>S. venezuelae</i> ATCC 10712	1	16
<i>S. venezuelae</i> pIJ10257	2	8
<i>S. venezuelae</i> pIJ-EnC	2	4
<i>S. venezuelae</i> pIJ-Enu	2	4
<i>S. venezuelae</i> pIJ-COM	2	8
<i>S. coelicolor</i> M1154	16	16
<i>S. coelicolor</i> pIJ	16	16
<i>S. coelicolor</i> pIJ-EnC	32	64
<i>S. coelicolor</i> pIJ-Enu	4	4
<i>S. coelicolor</i> pIJ-COM	4	8

Dr. Min Xu created the liquid MIC protocol for *Streptomyces*. The protocol involves growing overnight cultures from spore stocks and then diluting the mycelium to a final concentration of 1:400. While the protocol worked, it was difficult to have consistency with the results, as *Streptomyces* species clump as they grow, making dilutions less homogenous. One consistent factor across all attempts was that the MICs for the exconjugants containing parts or all the putative resistance cassettes did not significantly increase compared to empty vector and

wild-type strain controls. If there was more than a 2-fold increase in resistance, this would only be seen in one of two duplicates.

Solid MICs were attempted on Bennett’s agar to address the consistency issue with the liquid MICs. This involved taking 5 µL of treated cells from liquid MIC assays, and plating them onto Bennett’s agar, and letting these grow for two days. Solid MIC values were similar to the liquid MICs, with perhaps a slight increase on solid medium (Table 2-2).

Table 2-2. MICs of *Streptomyces* on solid media. Solid MICs were performed on Bennett’s agar in duplicate for both *Streptomyces* species. The number refers to the concentration of merolectin antibiotic in µg/mL at which cells did not grow. If one duplicate grew at a higher concentration than the other, that was taken as the MIC value.

	Complestatin	Enugumycin
<i>S. venezuelae</i>	4	64
<i>S. venezuelae pIJ</i>	8	8
<i>S. venezuelae pIJ-EnC</i>	8	8
<i>S. venezuelae pIJ-Enu</i>	8	8
<i>S. venezuelae pIJ-COM</i>	8	8
<i>S. coelicolor</i>	64	16
<i>S. coelicolor pIJ</i>	16	16
<i>S. coelicolor pIJ-EnC</i>	64	64
<i>S. coelicolor pIJ-Enu</i>	8	16
<i>S. coelicolor pIJ-COM</i>	16	16

These results show that these exconjugants are not resistant to meroctin antibiotics. Each of these exconjugants has been tested for proper integration of the plasmid into the chromosomal DNA of the two *Streptomyces* species (Appendix 4), and these genes are under a strong constitutive promoter. Therefore, we inferred that it is unlikely that the function of these genes is to confer resistance to these antibiotics.

While these findings discourage the possibility that these genes confer resistance to meroctin antibiotics, the resulting proteins from the putative resistance core and the putative TCS could physically interact with each other, as seen in the BceRS-AB system. Thus, to induce resistance, this interaction would be necessary. However, several thousand nucleotide base pairs separate the TCS in some of these conserved cassettes.

2.3.3 Assessment of Phenotypic Changes Induced by Meroctin Antibiotics

Different concentrations of the meroctin complestatin were assessed for potential phenotypic change in the cell shape of *Streptomyces*. There is no observable change in cell shape in wild-type *S. coelicolor* with the treatment of meroctins at 100 × magnification (Figure 2-2). As there was no difference in cell phenotype with meroctin treatment, and the MICs for the *S. coelicolor* exconjugants were not increased, further study of *S. coelicolor* was discontinued. As *S. coelicolor* has a higher MIC, it is possible that the distinct phenotype seen in *B. subtilis* cannot be observed unless the strains are more susceptible to the drug. An explanation for this lack of change in cell shape could involve the difference in cell structure in *S. coelicolor*. *Streptomyces* are known to be much more robust organisms that need more effort to break apart while isolating genomic materials. Thus, perhaps meroctins are not able to bind as easily to the peptidoglycan of *Streptomyces*.

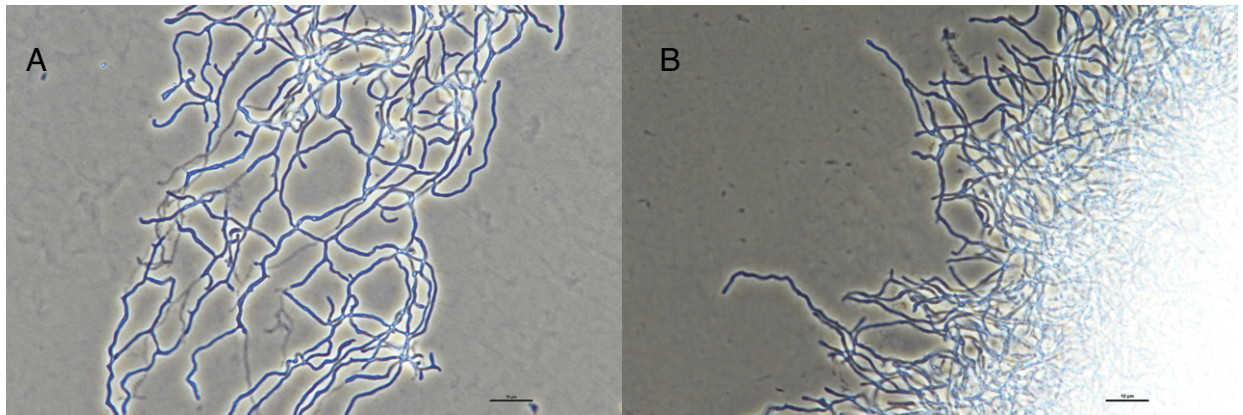


Figure 2-2. Light microscopy images from *S. coelicolor* M1154 under the effects of murobactin antibiotics. Cells were treated with sub-MIC concentrations of the murobactin antibiotic complestatin. Images were taken at $100\times$ magnification under oil immersion. **A)** Wild-type *S. coelicolor* treated with DMSO, **B)** Wild-type *S. coelicolor* treated with $0.5\times$ MIC complestatin.

In *S. venezuelae*, there seems to be a phenotypic change in cell shape and development in the treated versus untreated cells (Figure 2-3). The mycelia appear smaller and crumpled in the treated cells of *S. venezuelae* compared to the untreated; notably, the cells are found in more clumps, and there are instances of bulbar tips of the mycelia. The phenotype of the bulbar tips could align with the predicted mechanism of action for murobactin antibiotic, inhibiting autolysin activity and accumulating PG where biosynthesis is actively occurring.²⁹ The exconjugant pIJ-EnC appears healthier and the cells are more developed than the other strains. However, the untreated empty vector control resembles the other two exconjugant strains. This could indicate that with the putative resistance cassette, the cells can grow more robustly despite the presence of the murobactin.

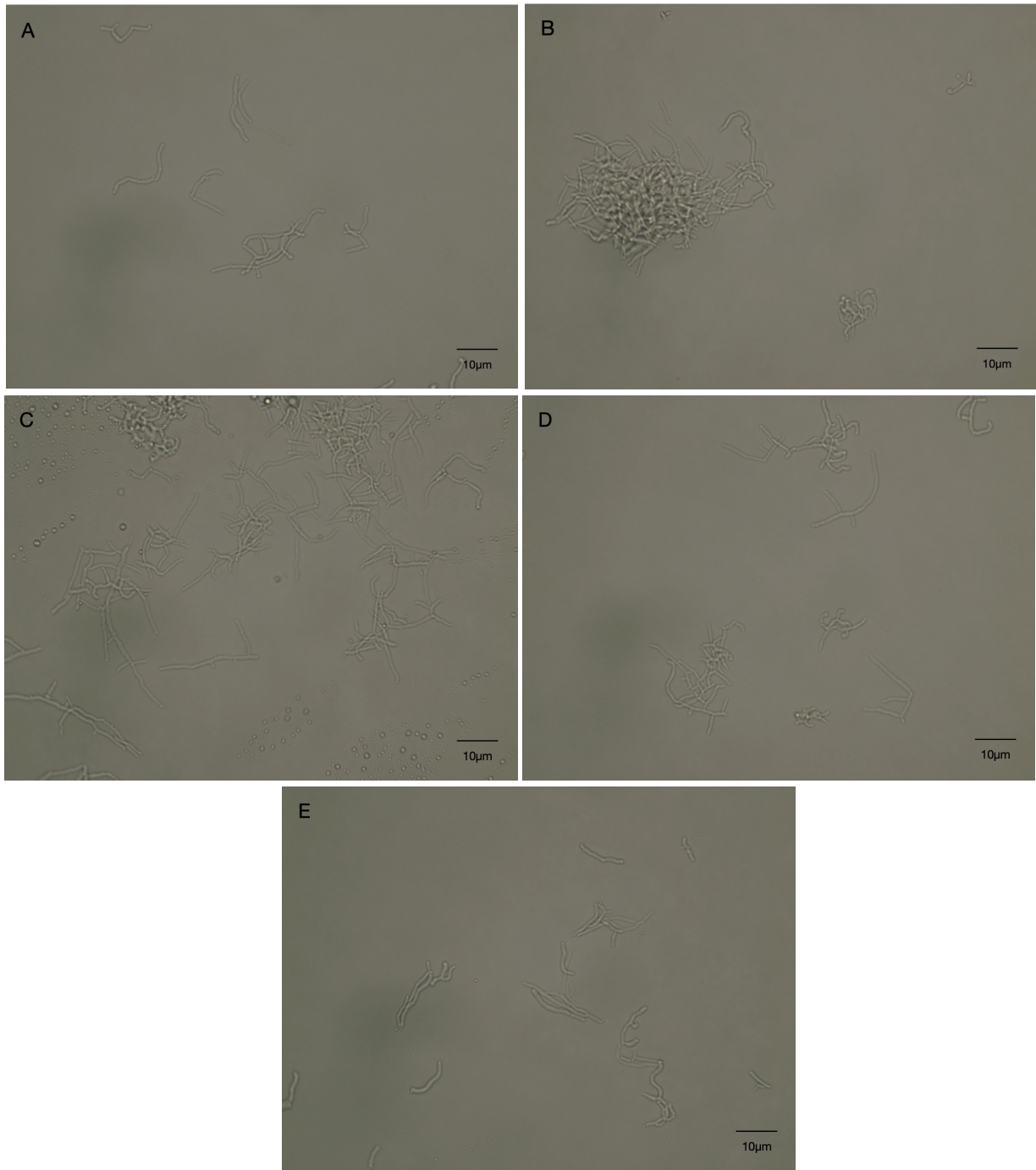


Figure 2-3. Light microscopy images from *S. venezuelae* pIJ10257, *S. venezuelae* pIJ-EnC, *S. venezuelae* pIJ-Enu, *S. venezuelae* pIJ-COM, under the effects of murobactin antibiotics. Cells were treated with sub-MIC concentrations of the murobactin antibiotic complestatin. Images were taken at 100× magnification under oil immersion. **A)** Empty vector control *S. venezuelae* pIJ10257 treated with DMSO, **B)** Empty vector control *S. venezuelae* pIJ10257 treated with $0.5 \times \text{MIC}$ complestatin, **C)** *S. venezuelae* pIJ-EnC treated with $0.5 \times \text{MIC}$ complestatin, **D)** *S. venezuelae* pIJ-Enu treated with $0.5 \times \text{MIC}$ complestatin, **E)** *S. venezuelae* pIJ-COM treated with $0.5 \times \text{MIC}$ complestatin.

2.3.4 Growth Curves & Assessment of Peptidoglycan Biosynthesis

Fluorescent D-amino acids (FDAAs) were used to assess peptidoglycan biosynthesis and observe where this process is takes place within the cell. The goal was to use this technique on cells treated with murebactins, however there was not sufficient time to explore this option. To use FDAAs efficiently, it was necessary to collect growth curve data from individual strains. *S. venezuelae* started to reach the exponential growth phase around six hours after incubation *S. coelicolor* took longer to reach this growth rate, at around eight hours (Figure 2-4). Strangely, after 24 hours, the OD₆₀₀ of these cells seem to drop. The cells may not have dispersed throughout the plate reader wells and may have aggregated to the bottom of the wells; thus, the machine could not take an accurate OD₆₀₀ reading.

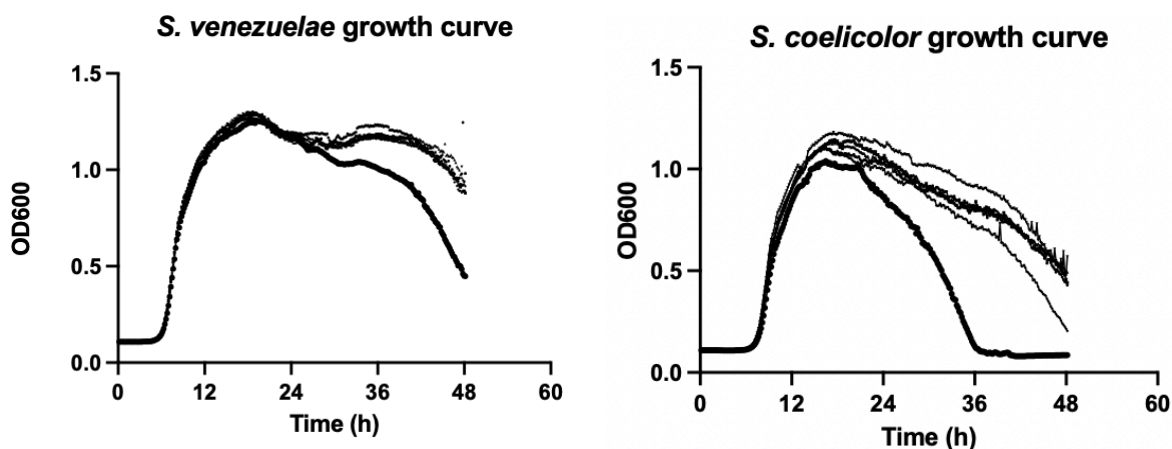


Figure 2-4. Growth curves of *Streptomyces* in plate reader. Growth curves of *S. venezuelae* and *S. coelicolor* at dilution of 1:400 from overnight culture. This was done in six replicates. OD₆₀₀ measurements were taken every 10 minutes for 48 hours. Every 12 hours of growth is labelled on the x-axis, and the OD to 1.5 is measured on the y-axis.

Manual growth curves (section 2.2.5) were also performed to confirm these results for the *Streptomyces* strains, as the OD₆₀₀ can get significantly higher than 1.0. The manual growth curve for *S. coelicolor* was not accurate, as the vegetative hyphae of this species are known to clump together. However, the growth curve for *S. venezuelae* was successful. These growth

curves were done starting with a dilution factor 1:50 from overnight culture, where the exponential growth started around 5 hours for *S. venezuelae*.

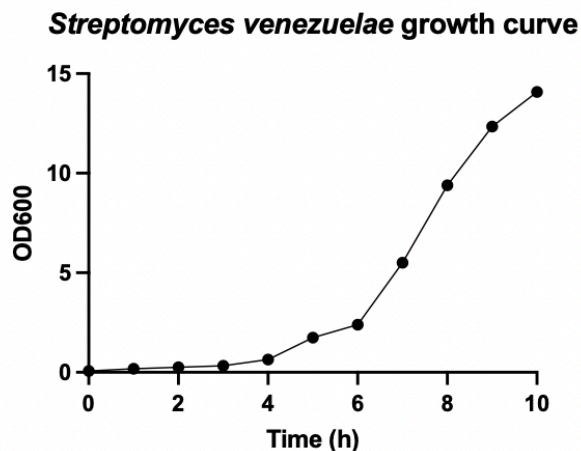


Figure 2-6. Manual growth curve of *S. venezuelae*. Growth curve of *S. venezuelae* at dilution of 1:50 in 100 mL flask of TSBY medium. OD₆₀₀ measurements were taken every hour for 10 hours.

Once growth data were collected, HADA (an FDAA) was used to assess PG biosynthesis in *S. venezuelae* (Figure 2-7). Fluorescence was seen in *S. venezuelae*; however, it was not at the tips of the mycelia but dispersed across the cells. During the protocol, the cells were not ethanol-fixed after being prepared for visualization under the microscope, as we hoped to visualize them with the agarose pad method described (2.2.4). Thus, the cells continued to grow while HADA was being washed off. This method could be used in the *Streptomyces* exconjugants, but ethanol fixation followed by the wash steps would be more efficient. However, there was not sufficient time to explore this experiment over others.

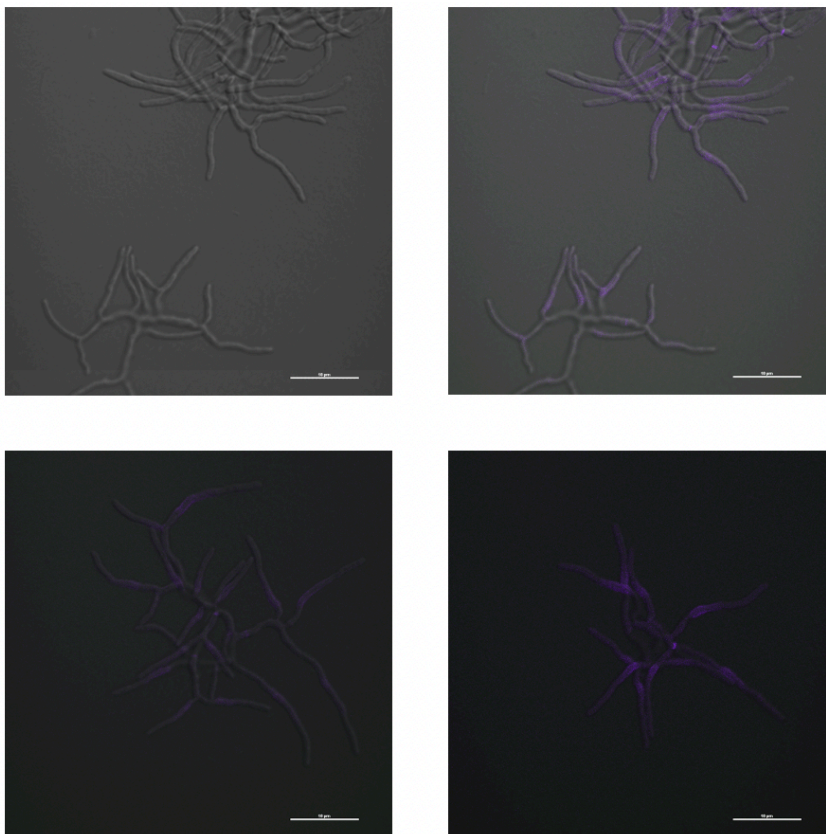


Figure 2-7. Fluorescence microscopy in *S. venezuelae*. Fluorescence microscopy was performed, and visualization was achieved using a DAPI laser with 500 μ M HADA (FDAA) cell treatment. Purple indicates the biosynthesis of PG.

2.3.5 Computational Analysis of Putative Resistance Genes

As the putative resistance core was seen in the BGCs of several muobactin-producing strains, it was intriguing to consider the possibility of these genes of interest being present in several other bacteria. With the help of Dirk Hackenberger, the core of this gene cluster (*enuUPEX*) was screened using cblaster to detect other homologues clustered closely together (Table 2-3). This list is significantly narrowed down; however, the entries show that different strains contain these six genes of interest clustered together. This analysis did not consider the presence of the rest of the muobactin BGC. The frequency of this gene cluster within several

species and strains of bacteria could imply that they are ancestors of an important system, whether that system be used to confer resistance or otherwise.

Table 2-3. cblaster results in non-*Streptomyces* organisms identifying the presence of the putative resistance cluster from the enugumycin producer. The score is based on a formula $S = h + i X s$ where h is the number of query sequences with BLAST hits, s is the number of contiguous gene pairs with conserved synteny, and i is a weighting factor (default value 0.5) determining the weight of synteny in the similarity score. *S. sp.* WAC 06738 (enugumycin producer) is the strain of interest, and this score is used as a reference point.

Organism	Score	enuU	enuP	enuE	enuX	enuR	enuS
<i>S. sp.</i> WAC 06738	11.3712	1	1	1	1	1	1
<i>Actinoplanes hulinensis</i> NEAU-M9	10.1763	1	1	1	1	1	1
<i>Micromonospora sp.</i> RD004123	10.1593	1	1	1	1	1	1
<i>Actinocatenispora</i> <i>thailandica</i> NBRC 105041	10.1584	1	1	1	1	1	1
<i>Plantactinospora</i> <i>alkalitolerans</i> S1510	10.1577	1	1	1	1	1	1
<i>Actinophytocola</i> <i>gossypii</i> S1-96	10.1567	1	1	1	1	1	1
<i>Rugosimonospora</i> <i>africana</i> NBRC 104875	10.1554	1	1	1	1	1	1

<i>Dactylosporangium sp.</i>							
AC04546	10.1549	1	1	1	1	1	1
<i>Kibdelosporangium</i>							
<i>banguiense</i> DSM 46670	10.1535	1	1	1	1	1	1
<i>Hamadaea sp.</i>	10.1507	1	1	1	1	1	1
<i>Kribbella sp.</i> VKM Ac-							
2569	10.1498	1	1	1	1	1	1
<i>Stackebrandtia</i>							
<i>nassauensis</i> DSM 44728	10.1497	1	1	1	1	1	1

Previously, I had shown a possible configuration of the protein complex containing EnuPEX. This configuration was based on the TolC efflux pump system, as part of EnuP resembles the adaptor protein in the complex MacA, which is known to connect the outer portion of the efflux pump to the inner portion.⁷⁷ Using AlphaFold 2.0, it was possible to predict the configuration of these proteins within a potential complex (Figure 2-8). Initially, the program was run with two copies of EnuE, two copies of EnuX, and one copy of EnuP. EnuU was also used in this program; however, it never fit within this complex. When run through a conserved domain database, the only recognizable sequence within EnuU is related to a signal sequence, possibly indicating that the protein is extracellular and not part of this complex. With one copy of EnuP, it appears as though another copy or several more copies could fit into the pocket created by EnuX. The program was run once again with two then four copies of EnuP.

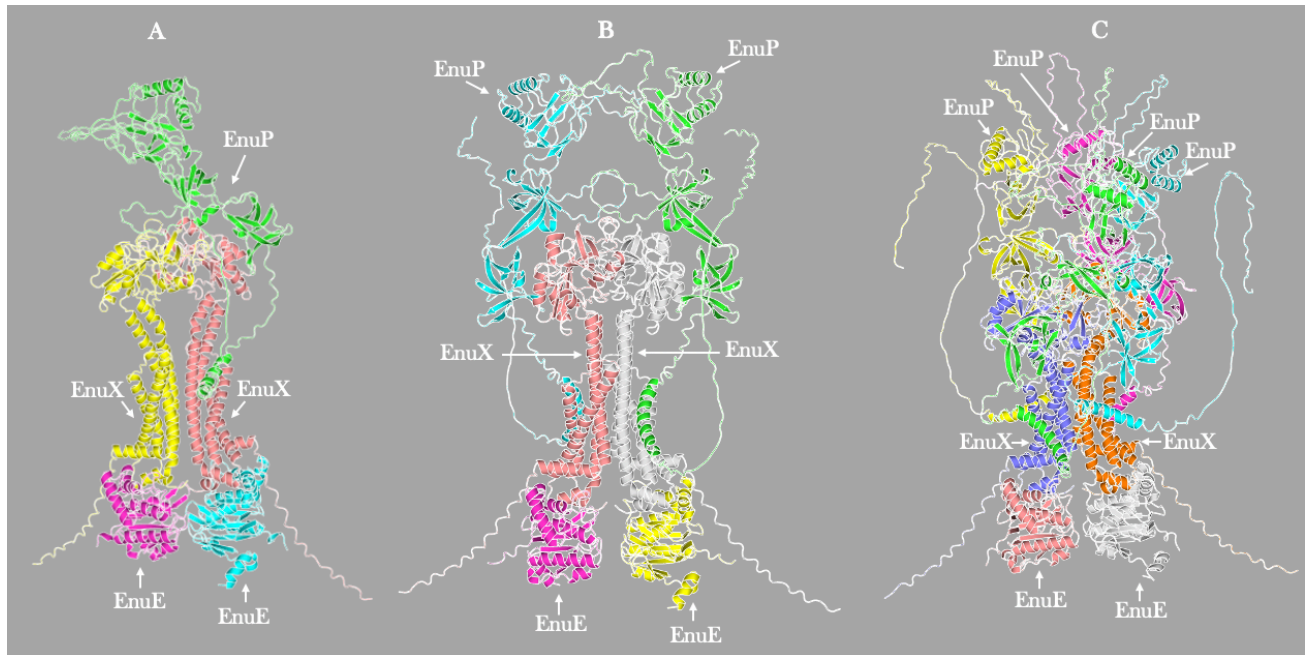


Figure 2-8. AlphaFold predictions of EnuPEX complex. A) AlphaFold prediction if only one EnuP protein were part of the complex. Hot pink & light blue = EnuE. Yellow & coral = EnuX. Green = EnuP. B) AlphaFold prediction with two EnuP. Hot pink & yellow = EnuE. Coral & grey = EnuX. Light blue & green = EnuP. C) AlphaFold prediction with four EnuP. Coral & grey = EnuE. Purple & orange = EnuX. Yellow, hot pink, green, and light blue = EnuP.

By using cblaster, it was possible to identify the genomic context surrounding the homologues of the *enuRSUPEX* cassette. Only Actinomycetota strains, which contained all parts of the putative resistance cassette, were included in this analysis. Overall, the genes surrounding this cassette do not show a consistent pattern. These genes are mostly of unknown function; however, two of the 52 samples have a predicted *chpC* gene, which is the gene that produces chaplin C (Figure 2-9). ChpC is a long chaplin which has two chaplin domains and a C-terminal “sorting signal” which sends them for attachment to the cell wall by sortase enzyme.

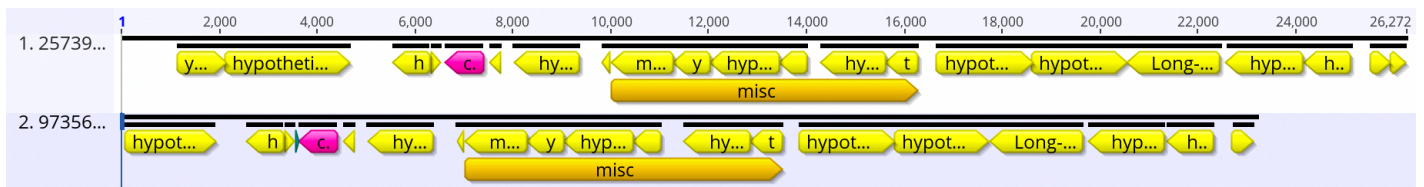


Figure 2-9. Genomic context of putative resistance genes. All yellow arrows represent different predicted genes; orange is the putative resistance cassette. These are the only 2 of 52 strains that contain *chpC* coloured in pink.

This could be due to the conservation of genome synteny instead of a confirmed pattern within the context of the genes. These two strains are very close together on a phylogenetic tree made from the context genes identified. Other than this, the genes surrounding the putative resistance cassette seem highly variable, such as NRPSs, cytochrome P450s, and DNA helicases.

2.3.6 RNA Isolation in *S. venezuelae*

RNA was isolated from these strains to perform RT-PCR and confirm if the genes of interest were being properly expressed in *S. venezuelae*. RNA extractions were done using the acid phenol-chloroform method. At first, there was excessive gDNA contamination; however, by adjusting methods and adding dsDNase, RNA was successfully extracted from *S. venezuelae* and exconjugants (Figure 2-10). At the top of the gels, gDNA is visible, though more importantly, there are evident bands for 23S rRNA and 16S rRNA, which indicates that the RNA is not degraded and is intact.

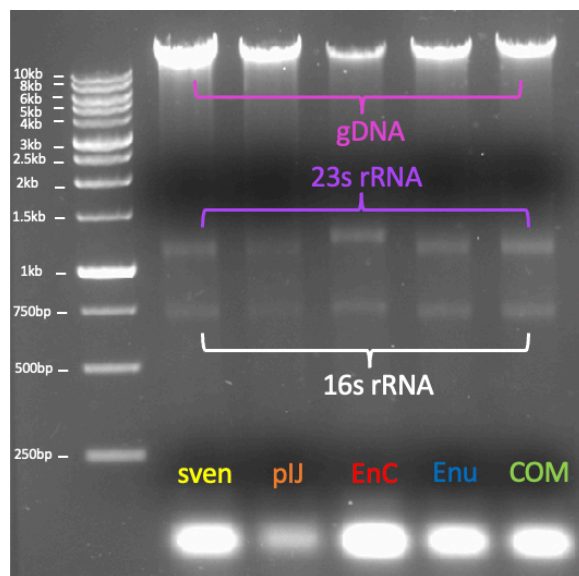


Figure 2-10. Gels of extracted RNA from *S. venezuelae*. *S. venezuelae* (sven), Pink = gDNA, purple = 23s rRNA, white 16s rRNA. Yellow = sven, orange = pIJ10257, red = pIJ-EnC, blue = pIJ-Enu, green = pIJ-COM.

2.3.7 RT-qPCR in *Streptomyces*

RT-qPCR was done to assess the gene transcription of our genes of interest. Primer binding efficiencies were calculated before performing RT-qPCR, all of which were 90%-110%. RT-qPCR was carried out for all exconjugants; pIJ-Enu, pIJ-EnC and pIJ-COM. *hrdB* was used as the housekeeping gene for *S. venezuelae*. Fold change was calculated for the three technical replicates from the Ct values; all no RT controls and NTCs were a Ct of 30 or below (Figure 2-11).

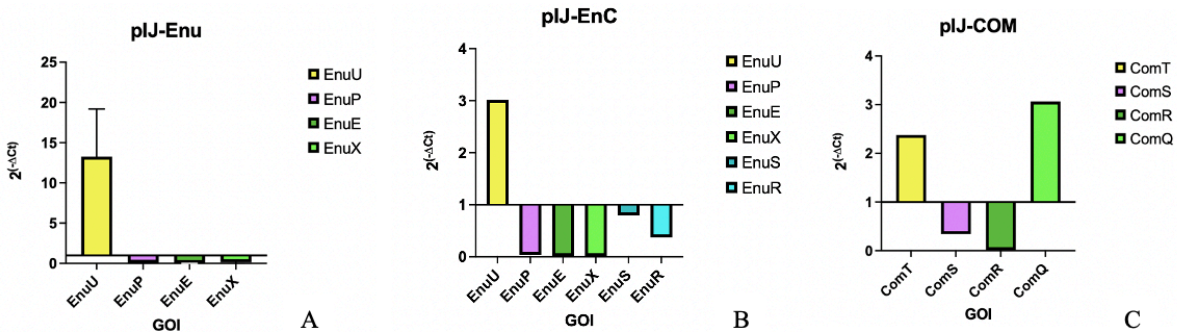


Figure 2-11. RT-qPCR results of pIJ-Enu, pIJ-EnC and pIJ-COM. Fold change is derived from Ct values (Ct (gene of interest) – Ct (housekeeping gene)). Homologous genes are represented by the same colour bar. Yellow = *enuU/comT*, purple = *enuP/comS*, dark green = *enuE/comR*, light green = *enuX/comQ*, dark turquoise = *enuS*, turquoise = *enuR*

As these genes are close together with no nucleotides between (save for the putative TCS in pIJ-EnC), it was assumed they were part of the same operon. However, the only gene upregulated was *enuU/comT* at the beginning of the operon and immediately next to the strong promoter *ermE**. One exception is *comQ* at the end of the predicted operon from the complestatin producer. This result demonstrates that the genes are not properly expressed, and perhaps a stronger promoter must be inserted between each gene.

2.3.8 Sporulation Assay

A sporulation assay was created to assess the change in sporulation or spore phenotype when in the presence of a murebactin and with the putative resistance genes. Initially, a sporulation assay was attempted, using a range of concentrations of complestatin (8-64 $\mu\text{g}/\text{mL}$) in *Streptomyces* minimal media (ISP4); however, no zone of inhibition was seen, and no change in spore phenotype. This experiment was then repeated to include 128 $\mu\text{g}/\text{mL}$ and 256 $\mu\text{g}/\text{mL}$. At both concentrations, the cells around the zone of inhibition were bright white compared to the spores on the rest of the plate (Figure 2-12A). This colour change is only seen in the wild-type, empty vector control, and pIJ-COM and is more pronounced in pIJ-COM. The white ring formed around the zone of inhibition could indicate a lack of efficient sporulation. However, this phenotype is visible as soon as mycelia grows on the plate. Notably, this phenotype is not seen in pIJ-Enu or pIJ-EnC. Therefore, only the two control strains and pIJ-COM were used to replicate the phenotype.

The sporulation assay was repeated on ISP4 and MYM plates. MYM plates were used as this is a nutrient-rich media for *S. venezuelae*. The concentrations of complestatin were increased, starting at 256 $\mu\text{g}/\text{mL}$ and ending at 2048 $\mu\text{g}/\text{mL}$, and the phenotype was much more obvious on ISP4 medium (Figure 2-12B). pIJ-COM exhibited a strong white ring and a slightly smaller zone of inhibition when compared to the control plates. However, on MYM plates, there was no indication of this phenotype. This result shows the phenotype is exclusive to a minimal nutrient environment. All samples were incubated at 30°C; when incubated at room temperature, this phenotype was either barely visible or not observed.

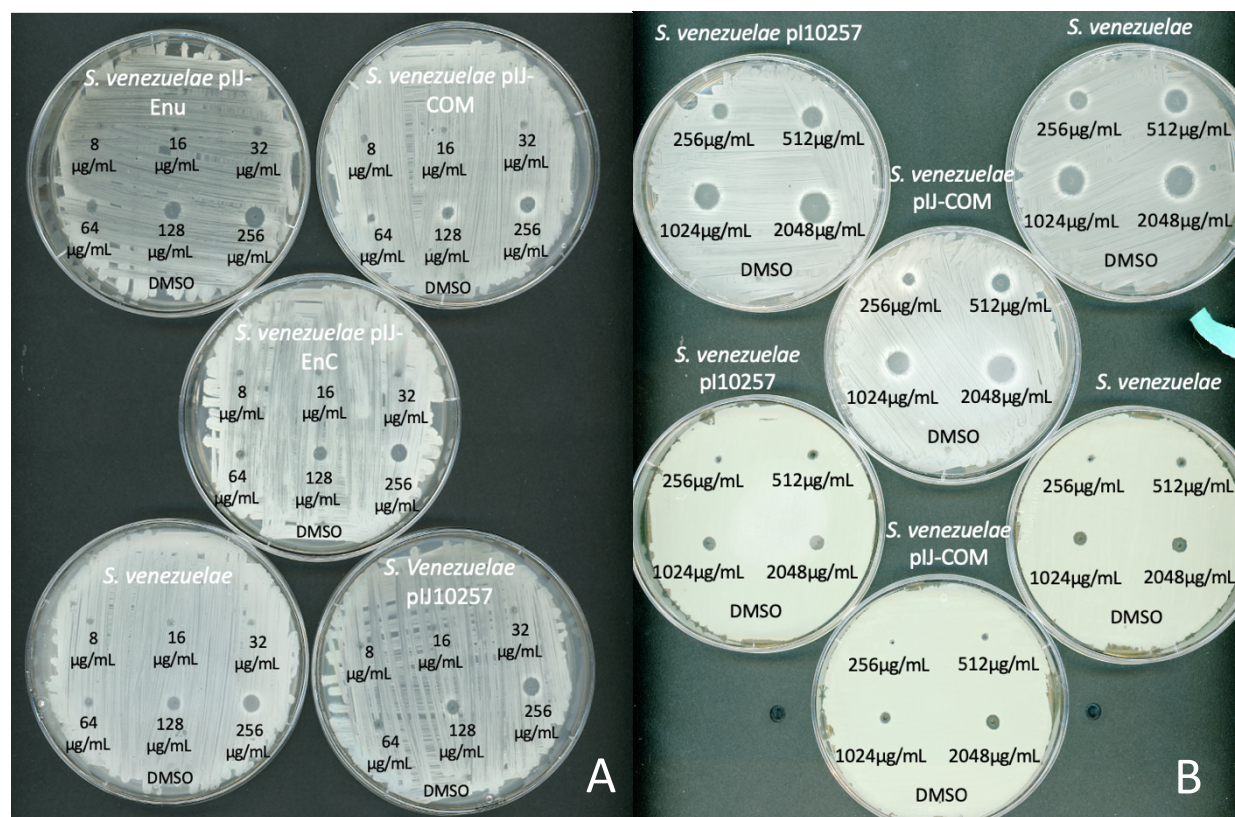


Figure 2-12. Sporulation assay on ISP4 and MYM plates. Strains are denoted on each plate, and each dot corresponds to an injection of 3 μL of the sample. DMSO was used as a control spot. **A)** Sporulation assay was done on ISP4 plates. A white ring around the zone of inhibition is seen at 128 $\mu\text{g/mL}$ and 256 $\mu\text{g/mL}$ in *S. venezuelae*, pIJ10257, and pIJ-COM. **B)** Sporulation assay was done on ISP4 (top three plates) and MYM plates (bottom three plates), at the bottom. Concentrations were increased (256 $\mu\text{g/mL}$ -2048 $\mu\text{g/mL}$). pIJ-COM exhibits a strong white ring and a slightly smaller zone of inhibition when compared to the control plates. On MYM plates, there is no indication of this phenotype.

2.3.9 MICs of Murobactins in Wright Actinomycetes Collection strains

MICs were performed for several WAC strains (Table 2-4). Using bioinformatics, strains from the Wright Actinomycete collection (WAC) were identified with the putative resistance cassette but without the biosynthesis machinery required to form murobactins. Next, WAC strains that did not have the putative resistance cassette or the biosynthesis machinery for murobactins were identified. Twelve strains were examined against the murobactin antibiotic complestatin, and *S. venezuelae* was used as a reference point for a susceptible strain.

It was expected that if the cassette truly confers resistance to murobactins, the MIC of cassette-containing strains would be significantly increased compared to those without the biosynthesis machinery or the putative cassette. Murobactin-producers were also included, as typically, the producing strain of an antibiotic would also house a resistance mechanism against said antibiotic. In this case, the murobactin producers were not inherently resistant to complestatin; the highest MIC seen was in WAC 6738 at 64 $\mu\text{g/mL}$. None of the strains with only the putative resistance genes conferred resistance to complestatin. When compared to *S. venezuelae*, only two exhibited higher MICs. All MICs were done in duplicate and were consistent across duplicates.

These results suggest that these genes do not confer resistance to murobactin antibiotics. These MIC studies also demonstrate that the producers are not inherently resistant to these antibiotics. This begs the question of whether these compounds are even antibiotics. As the mechanism of action for these compounds is so different from any other documented antibiotic, and when exposed to murobactins, producers cannot survive in elevated concentrations, it could be possible that murobactins have an antibiotic effect when pure. Chaplin proteins could be a close approximation to the action of these antibiotics, as these are small hydrophobic proteins that coat the cell to assist in the formation of aerial hyphae, and importantly, these proteins are toxic to cells at high doses.⁷⁸

Table 2-4. MICs of WAC strains. MICs were performed in SAM in duplicate for WAC strains and *S. venezuelae*. The number refers to the concentration of antibiotic (complestatin) in µg/mL at which cells did not grow. The grey bracket highlights murobactin non-producers, murobactin producers are highlighted by the blue bracket, and strains with only the putative resistance cassette are highlighted by the orange bracket.

	Strain	Complestatin MIC (µg/mL)
	<i>S. venezuelae</i>	2
Murobactin non-producers	WAC 5467	4
	WAC 5374	4
	WAC 4040	4
	WAC 8267	8
Murobactin producers	WAC 6738	64
	WAC 1325	16
	WAC 1529	4
	WAC 631	4
w/ putative resistance genes w/o biosynthesis	WAC 4247	16
	WAC 10734	1
	WAC 6891	2
	WAC 7264	16

2.3.10 Metagenomic Library Preparation of eDNA with FatI Partial Digestion

An alternative strategy to identify the resistance mechanism for murobactin was to use metagenomic libraries to identify candidate resistance genes within environmental soil. eDNA was isolated from soils in our large collection. Seven soils were chosen: United States, Nigeria, France, and four locations in Canada (Manitoba, Holman Island, Nova Scotia, and Hamilton, Ontario). eDNA was successfully isolated from all samples, and the DNA concentration in newer soil samples was elevated compared to older samples. Using FatI, eDNA was digested to the point of a visible “smear” on the gel. For 1 μg of sample, this appeared at the 50-minute mark, although 55-60 minutes was used due to the “smear” being brighter (Figure 2-12).

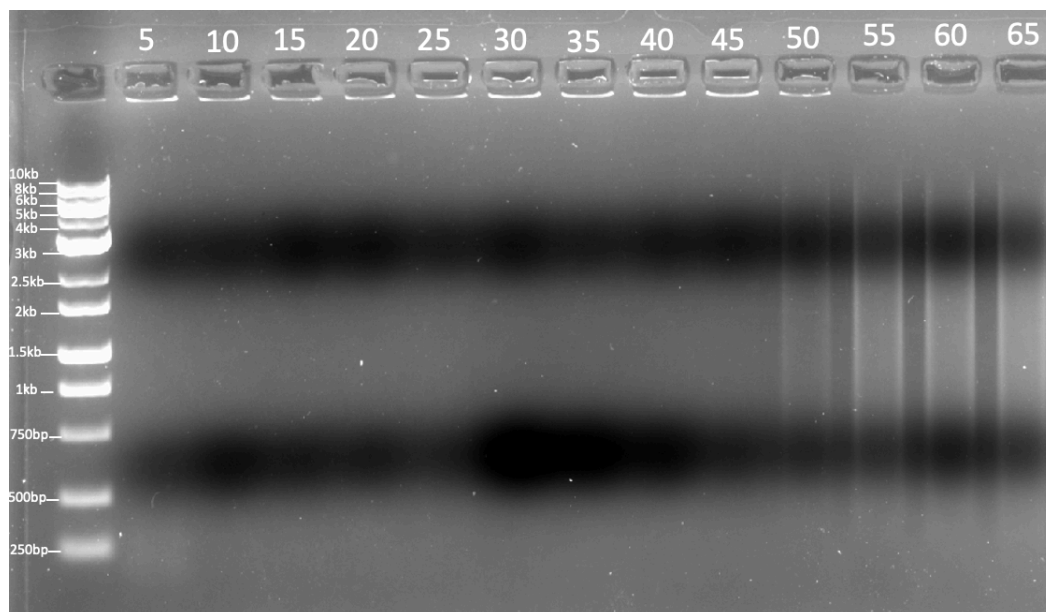


Figure 2-12. Visualizing partial digestion with FatI. Time points were taken every five minutes (amount of minutes is indicated at the top of the gel) to confirm when the digestion of the eDNA gave a visible smear on the gel; 1 μg of eDNA was digested.

From here, samples were first extracted using gel purification from the 1-5kb range to the 1kb range; however, the yield was too low for transformation into *E. coli* DHB10. The ligation of pUCXMG and the partially digested eDNA was done with a 3:1 and 2:1 molar ratio and left overnight at 4°C. Transformation in *E. coli* DH10B electrocompetent cells was performed and

plated on LB plates impregnated with a control antibiotic (10 µg/mL azithromycin), to assess the efficiency of the metagenomic library preparation and subsequent ligation. Azithromycin is known to have many antibiotic-resistance enzymes; however no cells grew. Cells did grow on plates with only the selection marker for the plasmid pUCXMG. This shows an issue with the ligation and not the competent cells.

The goal, then, was to obtain a higher concentration of eDNA to use a 10:1 molar ratio in the ligation reaction. Using Kapa Pure Beads, the concentration was similar to the gel purification; glass wool purification was also attempted but had an insufficient yield to achieve this molar ratio. Currently, this is the furthest this research has gone.

The bacterial host is an issue that needs to be addressed if this method is to be used to uncover the murobactin resistance mechanisms. Traditionally, *E. coli* is used to house metagenomic libraries. However, this bacterium is insensitive to murobactin antibiotics, and the library must be moved into a susceptible host such as *B. subtilis*.

Chapter 3: Assessing a Putative Resistance Mechanism Using *B. subtilis* as a Host

3.1 Introduction

In the paper by Culp et al.²⁹ – out of the Wright Lab – the phenotype of elongated cells treated with murebactins was observed in *B. subtilis*. As the most well-studied Gram-positive organism, *B. subtilis* can be used to understand how murebactin antibiotics work. Since the effect of murebactins on cell shape is prominent in this bacterium, it is a great candidate for expressing the putative resistance genes. This host is also known to be naturally competent; thus, transforming a plasmid containing the genes of interest is possible and reasonably straightforward. The next step in this research was to introduce these genes into the genome of *B. subtilis* and treat these strains with murebactins, where there should be an observable restoration of the “typical” cell shape.

3.2 Materials & Methods

3.2.1 pSWEET Constructs

The plasmid pSWEET-bgaB was isolated and prepared as previously described for pIJ10257 and was digested using the restriction enzymes PacI and NheI.⁷⁹ The same methodology was used for primer development, ligation, and transformation, using ampicillin (50 µg/mL) first, then chloramphenicol (10 µg/mL) as a selection marker (section 2.2.1).

3.2.2 Transformation of *B. subtilis*

An overnight culture of *B. subtilis* 168 was prepared in LB at 37°C. ST base (Appendix 1) was prepared before making competent cells for use in other solutions. Fresh medium (15 mL) known as SM1 (Appendix 1) was pre-warmed in a 125 mL flask was inoculated with 1 mL of overnight culture. The culture flask was incubated at 37°C until the culture reached the stationary phase. Measurements of the OD₆₀₀ were taken every hour by diluting the culture in 1:4 aliquots with fresh medium. An equal volume of SM2 (Appendix 1) was added, and the flask was

incubated for 90 minutes. The cell mixture was aliquoted into 500 μL volumes, flash-frozen in liquid nitrogen, and stored at -80°C until needed. Competent cells were incubated at 37°C for 30 minutes. For transformation, 5 μL of the desired plasmid was introduced to competent cells. LB media (300 μL) was added to the mixture and incubated for 30 minutes at 37°C . Cells were plated on LB selective media (chloramphenicol, 10 $\mu\text{g}/\text{mL}$).

3.2.3 MICs of Murobactins in *B. subtilis*

B.subtilis 168, *B.subtilis* pSWEET-bgaB, and *B.subtilis* pSWEET-COM were streaked onto plates with chloramphenicol (10 $\mu\text{g}/\text{mL}$) and incubated overnight at 30°C . Colonies were collected and diluted to $\text{OD}_{600}\sim 0.1$ in saline, then to 1:200 in LB. This was considered the cell and media mixture and was used directly in MIC plating. Stocks of antibiotics were made in DMSO as described for *Streptomyces* MICs. The antibiotic and media mixture (50 μL) and cell and media mixture (50 μL) were introduced into a fresh 96-well plate, and all assays were done in duplicate as previously described in section 2.2.3. Xylose (4%) was added to a final cell dilution following plating of no-xylose control, giving a final concentration of 2% xylose when plated with the antibiotic mixture. Xylose in this case, worked as an inducer for gene transcription of the putative resistance genes. Plates were incubated at 30°C overnight.

3.2.4 Assessment of Phenotypic Changes Induced by Murobactin Antibiotics

Samples were collected from MIC plates for microscopy. The methodology for visualizing cells with agarose pads was used for this experiment, as described in section 2.2.4.

The phenotypic change in *B. subtilis* was also assessed with a Gram stain to provide contrast when looking at the cells. Saturated *B. subtilis* from MIC plates (5 μL) was placed onto a microscope slide, and then all steps of a Gram stain were performed. The slides were visualized by light microscopy.

3.2.5 Growth Curve of *B. subtilis* & Assessment of Peptidoglycan Biosynthesis

The same methodologies previously described in sections 2.2.5 And 2.2.6 were used to capture the full growth curve of *B. subtilis* and introduce FDAAs to the growing PG of *B. subtilis*.

3.2.6 RNA Isolation in *B. subtilis* & cDNA Synthesis

Fresh LB (100 mL) was inoculated with 1:50 dilution of overnight culture. Cells were harvested via centrifugation and collected in 15 mL falcon tubes, spun down 4000 rpm for 10 mins at 4°C, and the supernatant was removed. Cells were flash-frozen in liquid nitrogen until needed. Cells were resuspended with 1M Tris-HCl (pH 7.5), and lysozyme was added to a final concentration of 10 mg/mL in a total volume of 300 µL. The mixture was incubated at 37°C for 30 minutes. Following incubation, the subsequent steps of RNA isolation follow those previously described in Chapter 2.

3.2.7 RT-qPCR in *B. subtilis*

Reverse Transcriptase quantitative PCR was performed with SYBR Select Master Mix CFX (Applied Sciences) on a Bio-Rad C1000 thermocycler as described in section 2.2.10. Expression was reported as a fold change using the housekeeping gene *yoxA* as a reference.

3.3 Results & Discussion

3.3.1 pIJ10257 Constructs

The putative resistance genes were cloned into *B. subtilis*, this was done to see if when these genes were into the genome, whether or not the susceptible strain conferred resistance to muobactins. Restriction cloning was performed successfully for all three *Bacillus* constructs. Clones were grown in 50 µg/mL ampicillin in *E. coli* TOP10 chemically competent cells. Plasmids were digested similarly to the pIJ10257 constructs, using restriction enzymes NheI and PacI. Two clones of each construct with the visible dropout bands of ~4kb or ~6kb were sent for sequencing; no mutations were identified within the inserted genes (Figure 3-1). The pSWEET

constructs were transformed into *B. subtilis* on LB plates with chloramphenicol (10 µg/mL). No transformants grew on plates with constructs for pSWEET-EnC and pSWEET-Enu. The plasmid concentration was adjusted here, and the amount of chloramphenicol and ampicillin on the LB plates was increased; however, in several different conditions, the two constructs could not be integrated into *B. subtilis*. Possibly, the genes from the enugumycin-producer could have a toxic effect on the cell.

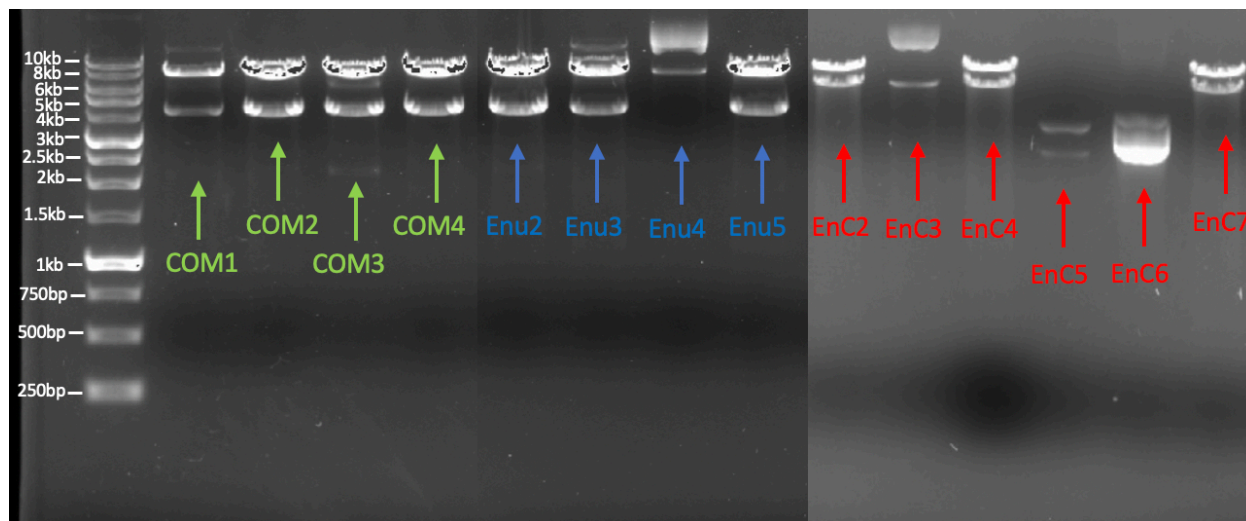


Figure 3-1. Isolated plasmid from *E. coli* TOP10 positive clones for pSWEET constructs containing genes of interest. pSWEET-EnC, pSWEET-Enu, pSWEET-COM were digested by NheI and PacI, yielding dropout bands ~6kb or ~4kb. Two of each construct were sent for plasmid sequencing.

3.3.2 MICs of Murobactins in *B. subtilis*

MICs were determined in *B. subtilis*, *B. subtilis* pSWEET-bgaB and *B. subtilis* pSWEET-COM (Table 3-1). This experiment was repeated twice, and all MICs were done in duplicate. These results were consistent; however, there was no significant change in MIC when comparing *B. subtilis* pSWEET-COM, the empty vector, and wild-type strains. These constructs are under an inducible promoter; thus, xylose was added to the cell suspension to ensure the expression of the genes of interest. These strains were also assessed for chromosomal integration, confirmed before these experiments (Appendix 4).

Table 3-1. MICs in *B. subtilis*. MICs were performed in LB in duplicate for *Bacillus* and transformants. This table displays the most recent results of these liquid MICs. OD₆₀₀ values were measured to confirm the MIC values in this table. The number refers to the concentration of antibiotic (murobactin) in µg/mL at which cells did not grow. If one duplicate grew at a higher concentration than the other, that was taken as the MIC value.

	No xylose		2% xylose	
	Complestatin (µg/mL)	Enugumycin (µg/mL)	Complestatin (µg/mL)	Enugumycin (µg/mL)
<i>B. subtilis</i> 168	4	2	4	4
<i>B. subtilis</i> <i>pSWEET-COM</i>	4	1	4	8
<i>B. subtilis</i> <i>pSWEET-bgaB</i>	4	1	8	4

While these genes were successfully integrated into the genome, it was possible that they were not being properly expressed in the host. This could be because the host has a lower GC content than the original producer strain. The phenotype of the cell shape was examined first in these strains despite the MIC results. RT-PCR was attempted after this visualization to see if these genes were being properly expressed. If the genes were not being transcribed successfully due to the high G+C content, the next step involved creating codon-optimized versions of these genes and cloning them into the integrative plasmid pSWEET to express in *B. subtilis*.

3.3.3 Assessment of Cell Shape Changes

Cells were treated with 2% xylose and 0.5 X MIC of the murobactin complestatin and visualized with light microscopy. Visualization was done using light microscopy, with the Gram stain procedure (Figure 3-2) and without this treatment (Figure 3-3). The empty vector control

strain appears filamentous at sub-MIC concentrations of the murobactin antibiotic complestatin. This phenotype has been previously seen in *B. subtilis* when treated with murobactins.²⁹ The strain containing the genes of interest (*B. subtilis* pSWEET-COM) lacks this kind of cell growth, possibly indicating the recovery of these cells from succumbing to the effects of murobactin antibiotics. Notably, this filamentous cell growth is not seen in the controls.

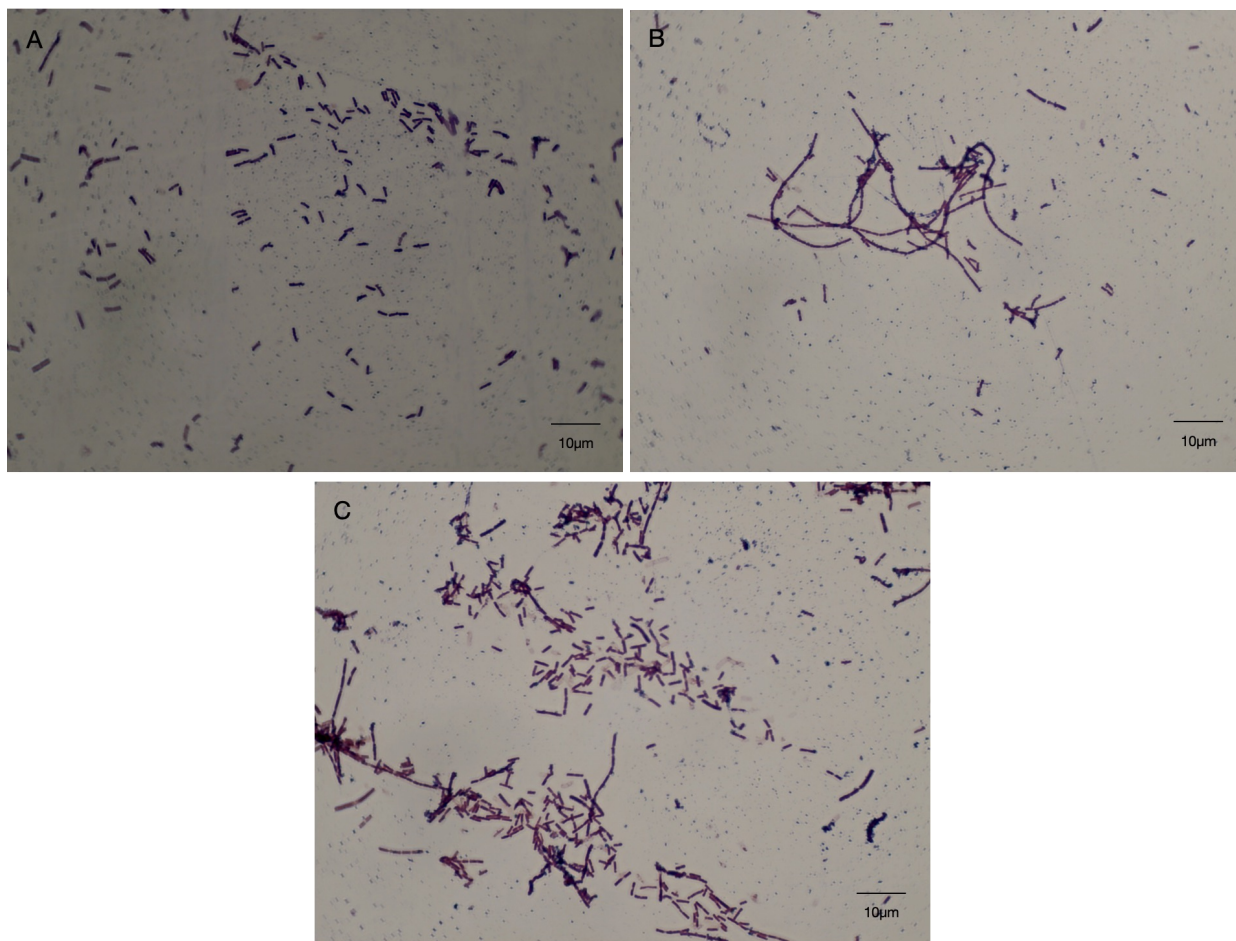


Figure 3-2. Gram-stained light microscopy images from *B. subtilis* pSWEET-bgaB and *B. subtilis* pSWEET-COM. Cells were treated with sub-MIC concentrations of the murobactin antibiotic complestatin and then Gram-stained. Images were taken at 100 × magnification under oil immersion. All cells were treated with 2% xylose for induction of the putative resistance genes. To confirm the inducer did not have a phenotypic effect on cells, the empty vector was also treated. **A)** Empty vector control *B. subtilis* pSWEET-bgaB treated with DMSO, **B)** Empty vector control *B. subtilis* pSWEET-bgaB treated with 0.5 × MIC complestatin, **C)** *B. subtilis* pSWEET-COM treated with 0.5 × MIC complestatin.

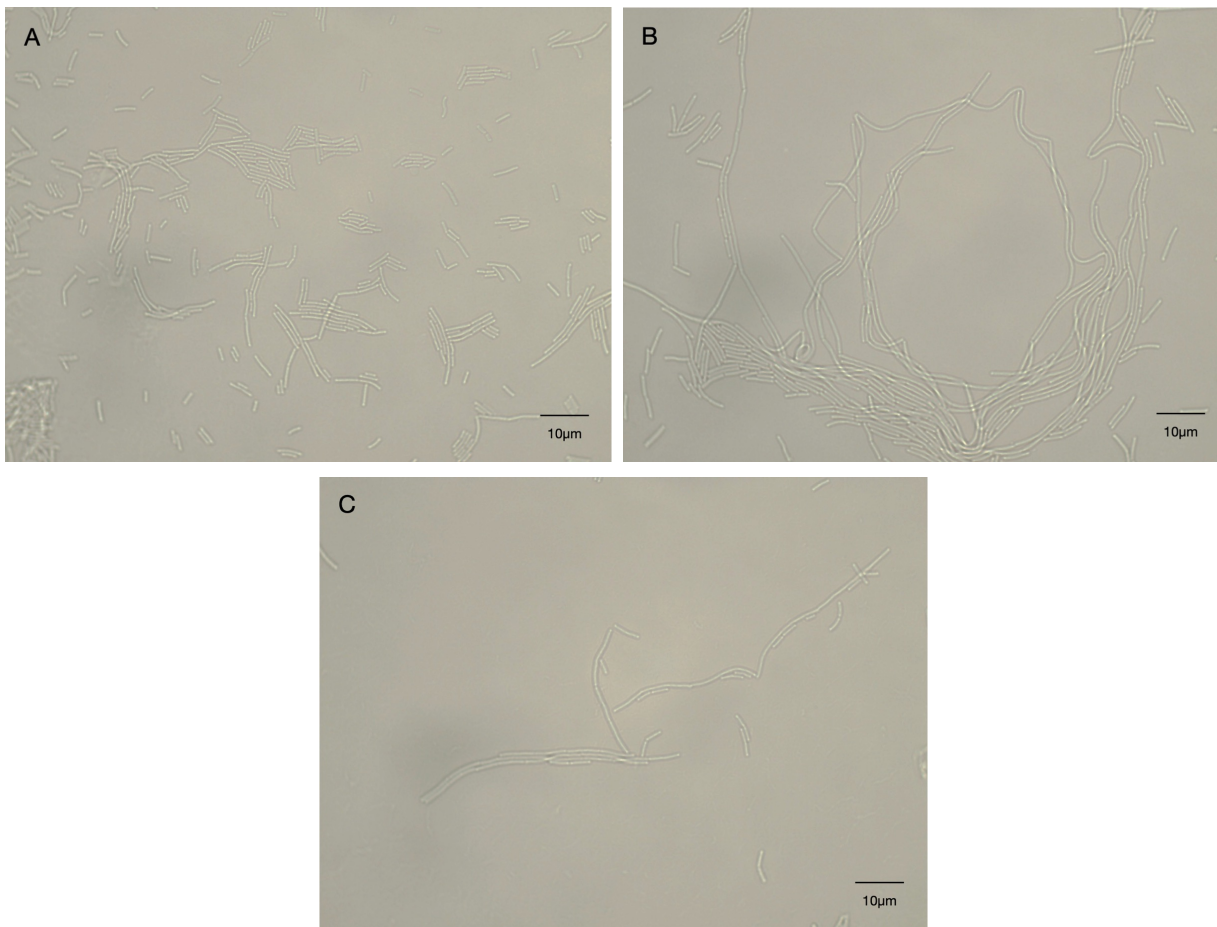


Figure 3-3. Light microscopy images from *B. subtilis* pSWEET-bgaB and *B. subtilis* pSWEET-COM. Treated with sub-MIC concentrations of the murebactin antibiotic complestatin. Images were taken at $100\times$ magnification under oil immersion. All cells were treated with 2% xylose for induction of the putative resistance genes. To confirm the inducer did not have a phenotypic effect on cells, the empty vector was also treated **A)** Empty vector control *B. subtilis* pSWEET-bgaB treated with DMSO, **B)** Empty vector control *B. subtilis* pSWEET-bgaB treated with $0.5\times$ MIC complestatin, **C)** *B. subtilis* pSWEET-COM treated with $0.5\times$ MIC complestatin.

3.3.4 Growth Curves & Assessment of Peptidoglycan Biosynthesis

FDAAs were used with *B. subtilis* as well, to assess peptidoglycan biosynthesis and ultimately to use this technique on cells treated with murebactins. The first step to using FDAAs *B. subtilis* growth curves were taken in a plate reader at a dilution factor of 1:400. *B. subtilis* reached the exponential growth phase around 10 hours after incubation (Figure 3-4). These

results were confirmed through manual growth curves. These growth curves were started using an overnight culture and diluting to 1:50 in 100 mL of fresh LB medium, where the exponential growth commences at 3-4 hours in *B. subtilis*.

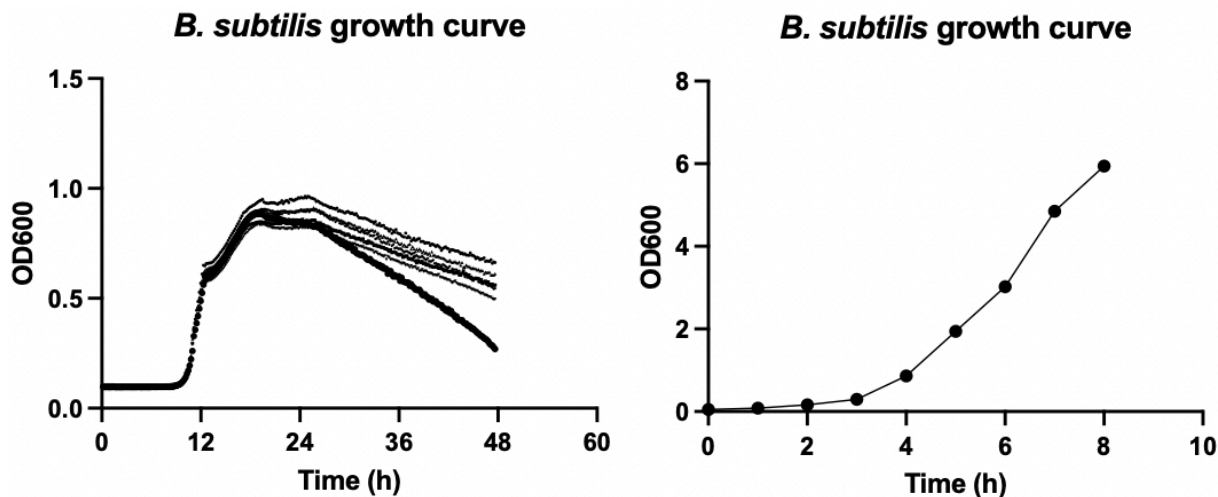


Figure 3-4. Growth curves of *B. subtilis* **A)** Growth curve of *B. subtilis* at dilution of 1:400 from overnight culture. This was done in six replicates. OD₆₀₀ measurements were taken every 10 minutes for 48 hours. **B)** Growth curve of *B. subtilis* at dilution of 1:50. OD₆₀₀ measurements were taken every hour for 10 hours.

Once growth data was collected, HADA (an FDAA) was used to assess PG biosynthesis in *B. subtilis* (Figure 3-5). Fluorescence was not seen in *B. subtilis*. During the protocol, the cells were not ethanol-fixed after they were prepared for visualization under the microscope. Notably, *B. subtilis* did not uptake any HADA; this could be due to the presence of DD-carboxypeptidases, which could have removed the incorporated FDAA before proper visualization.⁸⁰

B. subtilis



Figure 3-5. Fluorescence microscopy of *B. subtilis*. Fluorescence microscopy was performed, and visualization was achieved using a DAPI laser with 500 μ M HADA (FDAA) cell treatment. Purple indicates the biosynthesis of PG.

3.3.5 RNA Isolation in *B. subtilis* & cDNA Synthesis

RNA extraction was done using the acid phenol-chloroform method. The method was adapted from the RNA extraction protocol used for *Streptomyces* species. Cell pellets were extracted from 100 mL cultures with no treatment or 2% xylose introduced into the media. At the top of the gels, gDNA is visible, though more importantly, there are evident bands for 23S rRNA and 16S rRNA; this indicates that the RNA is not degraded and is intact (Figure 3-6). dsDNase was used to remove the gDNA in the sample when run on a gel; there appeared to be no gDNA, and RNA purity and integrity were maintained. However, it is important to note that gDNA could still be present in the RNA regardless of its absence in an agarose gel. cDNA was synthesized from isolated RNA, as described in the Methods section.

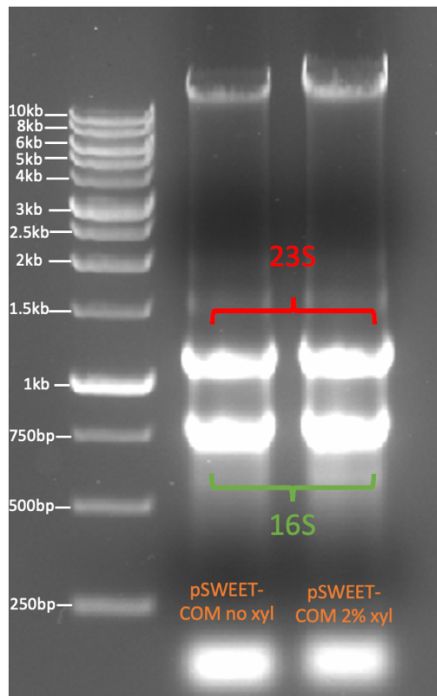


Figure 3-6. Gel of extracted RNA from *B. subtilis* 168 pSWEET-COM. Cells, when harvested, were treated with no xylose (no inducer) or 2% xylose to induce gene transcription. gDNA is present at the top of the gel. 23S rRNA and 16S rRNA bands are labelled. The gel is 1% agarose.

3.3.6 RT-qPCR in *B. subtilis*

B. subtilis pSWEET-COM was tested using a similar methodology described in the previous chapter. Here, the gene *yoxA* was used for the housekeeping reference.⁸¹ This has been attempted three times. In the first two, genomic DNA contamination was present in the no RT samples, but the NTCs did not exhibit this contamination, meaning the dsDNase portion of the cDNA preparation was the issue. The last time run, there was NTC contamination. These values were unusable due to these errors. Based on the weak cell shape phenotype in pSWEET-COM and considering the RT-qPCR results from *S. venezuelae*, we concluded that these genes may not be properly expressed in this host, and we decided to pursue codon optimization of the genes of interest.

3.3.7 Codon Optimization of Putative Resistance Genes for *B. subtilis*.

Codon optimization of the genes of interest was done using GenScript software. The putative resistance core from the complestatin producer was separated into three fragments. The goal was to reassemble these using Gibson assembly in the PSWEET vector. The construct was designed to have a strong constitutive promoter (P_{veg}) in place of an inducible promoter and to have a ribosomal binding site (RBS) in front of each gene of the putative resistance core. Gibson assembly was successful according to colony PCR at a 2:1 molar ratio of insert to vector (Figure 3-7). It is important to note that this colony PCR only used the primers for fragment 1; it is possible that these transformants did not possess all three fragments.

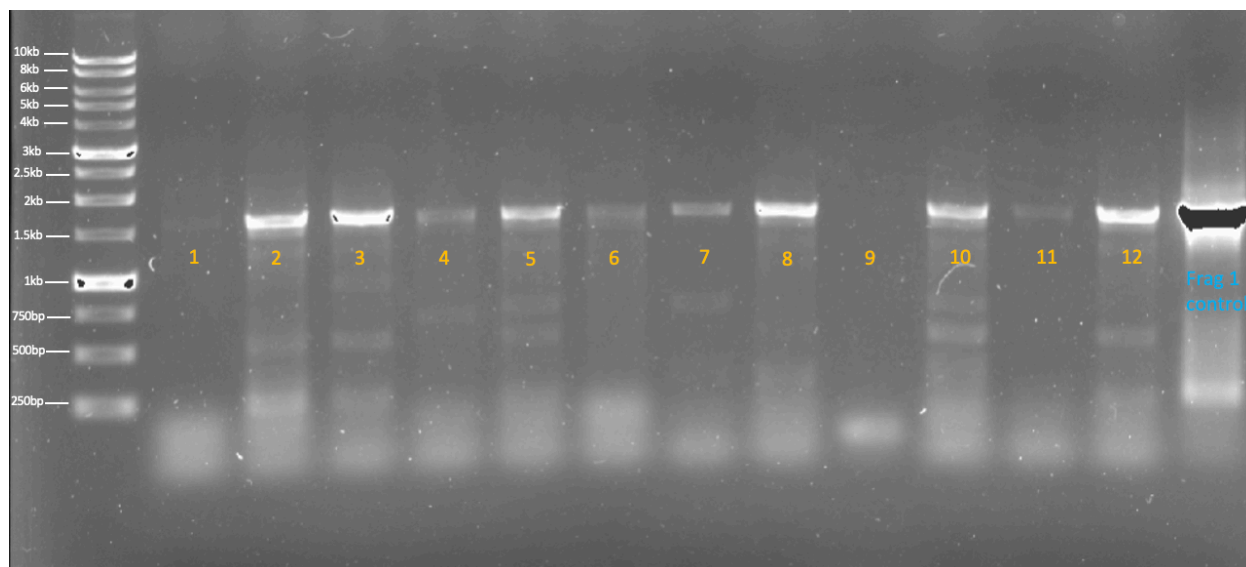


Figure 3-7. Colony PCR of pSWEET + codon-optimized genes. Colony PCR was performed with 12 transformants from plates with 100 $\mu\text{g}/\text{mL}$ ampicillin. Primers from fragment 1 were used in this reaction, and fragment 1 was used as a positive control.

When positive transformants were prepared in liquid media with the selection marker (100 $\mu\text{g}/\text{mL}$ ampicillin), they did not grow. Even when the amount of antibiotic was reduced to 50 $\mu\text{g}/\text{mL}$, the transformants could not grow. The isolation of this plasmid was even attempted

by streaking lawns of transformants on plates with the selection marker and taking up the cells by washing the plates with saline, but this was unsuccessful.

It is possible that these genes – when expressed – could be toxic to the cells, even though this was before its transformation into *B. subtilis*. As the promoter, in this case, is constitutive and can be expressed in *E. coli*, this supports the hypothesis that the expression of these genes is toxic to the cell. The construct was reworked to include a xylose-inducible promoter to hopefully control the expression of these genes if they were toxic. Gibson assembly was not successful with this construct. Multiple overlap extension PCRs were also attempted to try and assemble this construct, but this too was unsuccessful.

Chapter 4: Conclusions and Future Directions

This thesis aimed to identify a self-resistance mechanism for murobactin antibiotics. We believed that cloning the putative resistance cassette identified in murobactin-producers and introducing them into two different susceptible species would allow us to test their role in murobactin resistance. We were inclined to try alternative tests when it was shown through MIC testing that these strains containing the putative resistance cassette were not resistant to murobactins.

We assessed the phenotype of treated *S. venezuelae* exconjugants and *B. subtilis* transformant treated with complestatin and enugumycin. In *S. venezuelae pIJ-EnC*, there was a change in cell development compared to the empty vector control and the other exconjugants. In *B. subtilis*, there seemed to be a change in the cell shape of bacterial cells with the genes of interest present and with murobactin treatment. It was considered that these genes could have a hand in the cell division process.

The sporulation assay results, while puzzling, could provide some evidence for these genes lending a hand in the cell division process. The goal here was to identify a change in normal sporulation, and that did happen. Only at high concentrations of complestatin (minimum 128 µg/mL) was a bright white ring around the zone of inhibition. This ring appeared brighter on the plate with the complestatin genes incorporated into the genome. As the ring was much brighter and wider in the strains with the complestatin core genes, this means they enhanced this phenotype slightly. Upon further investigation through a time-lapse, this white band shows up simultaneously with the mycelia, showing that it could be a defect in spore formation or the attempt at forming aerial hyphae.

To test the hypothesis that these genes are involved in the cell division process of *Streptomyces* species, we could use fluorescently labelled murobactins such as corbomycin-BODIPY on *S. venezuelae* and the producer WAC strains to see where the antibiotic is localized. As murobactins are known to inhibit autolysin activity, the drug is localized only at the spots of autolysin activity, which is notably different in *Streptomyces* than in *B. subtilis*. This could help better understand the mechanism of action for this class of antibiotics and hypothesize how a resistance mechanism could work for these antibiotics.

It is important to reflect on the MIC testing of the WAC strains that produce murobactins. When exposed to the pure compound, even the producer organisms were susceptible to their corresponding antibiotic. This could imply that these compounds may not even be “antibiotics” per se. These compounds could have a similar effect as chaplins do in allowing aerial hyphae to escape the water but are potentially more localized to the sites of active cell division.

When performing computational analyses of this gene cluster, it was discovered that homologues to these four putative resistance core genes, along with the accompanying TCS, were present in several *Streptomyces* species and even species outside of the Actinobacteria phylum. At first, this gave us more confidence that these genes could be resistance markers for murobactin antibiotics, as this cluster could appear with or without the murobactin biosynthesis machinery. Looking back on these results and considering that these genes have not been shown to lend resistance to susceptible strains, this could be evidence that these genes are important and possibly essential to those strains that possess them; this comes back to the fact that these genes affect cell division in some way in the presence of murobactin antibiotics.

The genes of interest are significant to the mechanism of action for murebactins; however, at this point, I cannot be certain of the function(s) of these genes. Once a deletion mutant of the putative resistance genes in susceptible a *Streptomyces* species is confirmed, I would be interested in seeing its morphology without the genes and with murebactin treatment.

Some next steps could also involve the investigation of the TCS that often accompanies these genes. A bacterial two-hybrid assay could help confirm whether these proteins bind directly, though it is known that membrane-bound proteins are much more challenging to work within these experiments. Alternatively, experiments like those used in Wright et al., 1993 could test if murebactins activate the TCS and cause the upregulation of these genes of interest. However, this is only a fruitful avenue if we can confirm a distinct mechanism of action for the putative resistance core in the first place.

Through the experiments in this thesis, we have learned that these genes of interest do not lend resistance to susceptible strains. To identify the mechanism of resistance for these antibiotics, it would be best to confirm the molecular details of the mechanism of action of murebactin antibiotics. We have learned that homologues of this gene cluster are present in many species, giving them the potential to be genes related to an essential process. To identify an actual resistance enzyme or mechanism, we could continue to explore the metagenomic libraries in a Gram-positive host. However, it is important to consider that there may be no current resistance mechanism for these compounds as they may be more similar to chaplins or hydrophobins, and they may not be acting as antibiotics in the producing organisms.

ReferencesReferences

1. Armstrong, G.L., Conn, L.A., and Pinner, R.W. (1999). Trends in infectious disease mortality in the United States during the 20th century. *JAMA* *281*, 61-66. 10.1001/jama.281.1.61.
2. Carr, V.R., Shkoporov, A., Hill, C., Mullany, P., and Moyes, D.L. (2021). Probing the Mobilome: Discoveries in the Dynamic Microbiome. *Trends Microbiol* *29*, 158-170. 10.1016/j.tim.2020.05.003.
3. Martinez, J.L., Coque, T.M., Lanza, V.F., de la Cruz, F., and Baquero, F. (2017). Genomic and metagenomic technologies to explore the antibiotic resistance mobilome. *Ann N Y Acad Sci* *1388*, 26-41. 10.1111/nyas.13282.
4. Benveniste, R., and Davies, J. (1973). Aminoglycoside antibiotic-inactivating enzymes in actinomycetes similar to those present in clinical isolates of antibiotic-resistant bacteria. *Proc Natl Acad Sci U S A* *70*, 2276-2280. 10.1073/pnas.70.8.2276.
5. Cundliffe, E. (1989). How antibiotic-producing organisms avoid suicide. *Annu Rev Microbiol* *43*, 207-233. 10.1146/annurev.mi.43.100189.001231.
6. Marshall, C.G., Lessard, I.A., Park, I., and Wright, G.D. (1998). Glycopeptide antibiotic resistance genes in glycopeptide-producing organisms. *Antimicrob Agents Chemother* *42*, 2215-2220. 10.1128/AAC.42.9.2215.
7. McEwen, S.A., and Collignon, P.J. (2018). Antimicrobial Resistance: a One Health Perspective. *Microbiol Spectr* *6*. 10.1128/microbiolspec.ARBA-0009-2017.
8. Arnold, K.E., Laing, G., McMahon, B.J., Fanning, S., Stekel, D.J., Pahl, O., Coyne, L., Latham, S.M., and McIntyre, K.M. (2024). The need for One Health systems-thinking approaches to understand multiscale dissemination of antimicrobial resistance. *Lancet Planet Health* *8*, e124-e133. 10.1016/S2542-5196(23)00278-4.
9. Lobanovska, M., and Pilla, G. (2017). Penicillin's Discovery and Antibiotic Resistance: Lessons for the Future? *Yale J Biol Med* *90*, 135-145.
10. Rammelkamp, C.H., and Maxon, T. (1942). Resistance of *Staphylococcus aureus* to the Action of Penicillin. *Proceedings of the Society for Experimental Biology and Medicine* *51*, 386-389. 10.3181/00379727-51-13986.
11. Hutchings, M.I., Truman, A.W., and Wilkinson, B. (2019). Antibiotics: past, present and future. *Curr Opin Microbiol* *51*, 72-80. 10.1016/j.mib.2019.10.008.
12. Leclercq, R., Derlot, E., Duval, J., and Courvalin, P. (1988). Plasmid-mediated resistance to vancomycin and teicoplanin in *Enterococcus faecium*. *New England Journal of Medicine* *319*, 157-161.
13. Dhanda, G., Acharya, Y., and Haldar, J. (2023). Antibiotic Adjuvants: A Versatile Approach to Combat Antibiotic Resistance. *ACS Omega* *8*, 10757-10783. 10.1021/acsomega.3c00312.
14. Tu, M., Carfrae, L., Rachwalski, K., French, S., Catacutan, D., Gordzevich, R., MacNair, C., Speagle, M., Werah, F., Stokes, J., and Brown, E. (2023). The fitness cost of metallo- β -lactamase expression is a potential target for new therapeutic approaches to carbapenem resistance. 10.21203/rs.3.rs-3683698/v1.
15. Xu, M., Wang, W., and Wright, G.D. (2022). Glycopeptide antibiotic discovery in the genomic era. *Methods Enzymol* *665*, 325-346. 10.1016/bs.mie.2021.11.009.

16. Flardh, K., and Buttner, M.J. (2009). Streptomyces morphogenetics: dissecting differentiation in a filamentous bacterium. *Nat Rev Microbiol* 7, 36-49. 10.1038/nrmicro1968.
17. Petrus, M.L., and Claessen, D. (2014). Pivotal roles for Streptomyces cell surface polymers in morphological differentiation, attachment and mycelial architecture. *Antonie Van Leeuwenhoek* 106, 127-139. 10.1007/s10482-014-0157-9.
18. Elliot, M.A., and Talbot, N.J. (2004). Building filaments in the air: aerial morphogenesis in bacteria and fungi. *Curr Opin Microbiol* 7, 594-601. 10.1016/j.mib.2004.10.013.
19. Tillotson, R., Wösten, H., Richter, M., and Willey, J. (1998). A surface active protein involved in aerial hyphae formation in the filamentous fungus *Schizophyllum commune* restores the capacity of a bald mutant of the filamentous bacterium *Streptomyces coelicolor* to erect aerial structures. *Molecular microbiology* 30, 595-602.
20. Wösten, H.A. (2001). Hydrophobins: multipurpose proteins. *Annual Reviews in Microbiology* 55, 625-646.
21. Kershaw, M.J., and Talbot, N.J. (1998). Hydrophobins and repellents: proteins with fundamental roles in fungal morphogenesis. *Fungal Genetics and Biology* 23, 18-33.
22. Barka, E.A., Vatsa, P., Sanchez, L., Gaveau-Vaillant, N., Jacquard, C., Meier-Kolthoff, J.P., Klenk, H.P., Clement, C., Ouhdouch, Y., and van Wezel, G.P. (2016). Taxonomy, Physiology, and Natural Products of Actinobacteria. *Microbiol Mol Biol Rev* 80, 1-43. 10.1128/MMBR.00019-15.
23. Medema, M.H., Kottmann, R., Yilmaz, P., Cummings, M., Biggins, J.B., Blin, K., de Bruijn, I., Chooi, Y.H., Claesen, J., Coates, R.C., et al. (2015). Minimum Information about a Biosynthetic Gene cluster. *Nat Chem Biol* 11, 625-631. 10.1038/nchembio.1890.
24. Liu, R., Deng, Z., and Liu, T. (2018). Streptomyces species: Ideal chassis for natural product discovery and overproduction. *Metab Eng* 50, 74-84. 10.1016/j.ymben.2018.05.015.
25. Kwon, M.J., Steiniger, C., Cairns, T.C., Wisecaver, J.H., Lind, A.L., Pohl, C., Regner, C., Rokas, A., and Meyer, V. (2021). Beyond the Biosynthetic Gene Cluster Paradigm: Genome-Wide Coexpression Networks Connect Clustered and Unclustered Transcription Factors to Secondary Metabolic Pathways. *Microbiol Spectr* 9, e0089821. 10.1128/Spectrum.00898-21.
26. Shi, Y.M., Hirschmann, M., Shi, Y.N., Ahmed, S., Abebew, D., Tobias, N.J., Grun, P., Cramés, J.J., Poschel, L., Kuttlenlochner, W., et al. (2022). Global analysis of biosynthetic gene clusters reveals conserved and unique natural products in entomopathogenic nematode-symbiotic bacteria. *Nat Chem* 14, 701-712. 10.1038/s41557-022-00923-2.
27. Li, L., MacIntyre, L.W., and Brady, S.F. (2021). Refactoring biosynthetic gene clusters for heterologous production of microbial natural products. *Curr Opin Biotechnol* 69, 145-152. 10.1016/j.copbio.2020.12.011.
28. Johnston, C.W., Badran, A.H., and Collins, J.J. (2020). Continuous bioactivity-dependent evolution of an antibiotic biosynthetic pathway. *Nat Commun* 11, 4202. 10.1038/s41467-020-18018-2.
29. Culp, E.J., Waglechner, N., Wang, W., Fiebig-Comyn, A.A., Hsu, Y.P., Koteva, K., Sychantha, D., Coombes, B.K., Van Nieuwenhze, M.S., Brun, Y.V., and Wright, G.D. (2020). Evolution-guided discovery of antibiotics that inhibit peptidoglycan remodelling. *Nature* 578, 582-587. 10.1038/s41586-020-1990-9.

30. Tenconi, E., and Rigali, S. (2018). Self-resistance mechanisms to DNA-damaging antitumor antibiotics in actinobacteria. *Curr Opin Microbiol* 45, 100-108. 10.1016/j.mib.2018.03.003.
31. Schwarz, S., Kehrenberg, C., Doublet, B., and Cloeckert, A. (2004). Molecular basis of bacterial resistance to chloramphenicol and florfenicol. *FEMS Microbiol Rev* 28, 519-542. 10.1016/j.femsre.2004.04.001.
32. Murray, I.A., Gil, J.A., Hopwood, D.A., and Shaw, W.V. (1989). Nucleotide sequence of the chloramphenicol acetyltransferase gene of *Streptomyces acrimycini*. *Gene* 85, 283-291. 10.1016/0378-1119(89)90420-4.
33. Sundin, G.W., and Bender, C.L. (1996). Dissemination of the *strA-strB* streptomycin-resistance genes among commensal and pathogenic bacteria from humans, animals, and plants. *Mol Ecol* 5, 133-143. 10.1111/j.1365-294x.1996.tb00299.x.
34. Ogawara, H. (2015). Penicillin-binding proteins in Actinobacteria. *J Antibiot (Tokyo)* 68, 223-245. 10.1038/ja.2014.148.
35. Bakheet, T.M., and Doig, A.J. (2010). Properties and identification of antibiotic drug targets. *BMC Bioinformatics* 11, 195. 10.1186/1471-2105-11-195.
36. Vollmer, W., Blanot, D., and de Pedro, M.A. (2008). Peptidoglycan structure and architecture. *FEMS Microbiol Rev* 32, 149-167. 10.1111/j.1574-6976.2007.00094.x.
37. Cabeen, M.T., and Jacobs-Wagner, C. (2005). Bacterial cell shape. *Nat Rev Microbiol* 3, 601-610. 10.1038/nrmicro1205.
38. de Kruijff, B., van Dam, V., and Breukink, E. (2008). Lipid II: a central component in bacterial cell wall synthesis and a target for antibiotics. *Prostaglandins Leukot Essent Fatty Acids* 79, 117-121. 10.1016/j.plefa.2008.09.020.
39. Burman, L.G., and Park, J.T. (1984). Molecular model for elongation of the murein sacculus of *Escherichia coli*. *Proc Natl Acad Sci U S A* 81, 1844-1848. 10.1073/pnas.81.6.1844.
40. de Jonge, B.L., Wientjes, F.B., Jurida, I., Driehuis, F., Wouters, J.T., and Nanninga, N. (1989). Peptidoglycan synthesis during the cell cycle of *Escherichia coli*: composition and mode of insertion. *J Bacteriol* 171, 5783-5794. 10.1128/jb.171.11.5783-5794.1989.
41. Garde, S., Chodisetti, P.K., and Reddy, M. (2021). Peptidoglycan: Structure, Synthesis, and Regulation. *EcoSal Plus* 9. 10.1128/ecosalplus.ESP-0010-2020.
42. Vermassen, A., Leroy, S., Talon, R., Provot, C., Popowska, M., and Desvaux, M. (2019). Cell Wall Hydrolases in Bacteria: Insight on the Diversity of Cell Wall Amidases, Glycosidases and Peptidases Toward Peptidoglycan. *Front Microbiol* 10, 331. 10.3389/fmicb.2019.00331.
43. Heidrich, C., Templin, M.F., Ursinus, A., Merdanovic, M., Berger, J., Schwarz, H., de Pedro, M.A., and Holtje, J.V. (2001). Involvement of N-acetylmuramyl-L-alanine amidases in cell separation and antibiotic-induced autolysis of *Escherichia coli*. *Mol Microbiol* 41, 167-178. 10.1046/j.1365-2958.2001.02499.x.
44. Holtje, J.V. (1995). From growth to autolysis: the murein hydrolases in *Escherichia coli*. *Arch Microbiol* 164, 243-254. 10.1007/BF02529958.
45. Vollmer, W., Joris, B., Charlier, P., and Foster, S. (2008). Bacterial peptidoglycan (murein) hydrolases. *FEMS Microbiol Rev* 32, 259-286. 10.1111/j.1574-6976.2007.00099.x.

46. Sibirinelli-Sousa, S., Hespanhol, J.T., and Bayer-Santos, E. (2021). Targeting the Achilles' Heel of Bacteria: Different Mechanisms To Break Down the Peptidoglycan Cell Wall during Bacterial Warfare. *J Bacteriol* 203. 10.1128/JB.00478-20.
47. El Zoeiby, A., Sanschagrín, F., and Levesque, R.C. (2003). Structure and function of the Mur enzymes: development of novel inhibitors. *Molecular Microbiology* 47, 1-12. <https://doi.org/10.1046/j.1365-2958.2003.03289.x>.
48. Stone, K.J., and Strominger, J.L. (1971). Mechanism of action of bacitracin: complexation with metal ion and C 55 -isoprenyl pyrophosphate. *Proc Natl Acad Sci U S A* 68, 3223-3227. 10.1073/pnas.68.12.3223.
49. Binda, E., Marinelli, F., and Marcone, G.L. (2014). Old and New Glycopeptide Antibiotics: Action and Resistance. *Antibiotics (Basel)* 3, 572-594. 10.3390/antibiotics3040572.
50. Rubinstein, E., and Keynan, Y. (2014). Vancomycin revisited - 60 years later. *Front Public Health* 2, 217. 10.3389/fpubh.2014.00217.
51. Faron, M.L., Ledebøer, N.A., and Buchan, B.W. (2016). Resistance Mechanisms, Epidemiology, and Approaches to Screening for Vancomycin-Resistant Enterococcus in the Health Care Setting. *J Clin Microbiol* 54, 2436-2447. 10.1128/JCM.00211-16.
52. Bugg, T.D., Wright, G.D., Dutka-Malen, S., Arthur, M., Courvalin, P., and Walsh, C.T. (1991). Molecular basis for vancomycin resistance in *Enterococcus faecium* BM4147: biosynthesis of a depsipeptide peptidoglycan precursor by vancomycin resistance proteins VanH and VanA. *Biochemistry* 30, 10408-10415. 10.1021/bi00107a007.
53. Arthur, M., Reynolds, P., and Courvalin, P. (1996). Glycopeptide resistance in enterococci. *Trends Microbiol* 4, 401-407. 10.1016/0966-842x(96)10063-9.
54. Yim, G., Thaker, M.N., Koteva, K., and Wright, G. (2014). Glycopeptide antibiotic biosynthesis. *J Antibiot (Tokyo)* 67, 31-41. 10.1038/ja.2013.117.
55. Meziane-Cherif, D., Saul, F.A., Haouz, A., and Courvalin, P. (2012). Structural and functional characterization of VanG D-Ala:D-Ser ligase associated with vancomycin resistance in *Enterococcus faecalis*. *J Biol Chem* 287, 37583-37592. 10.1074/jbc.M112.405522.
56. Kwun, M.J., Novotna, G., Hesketh, A.R., Hill, L., and Hong, H.-J. (2013). In vivo studies suggest that induction of VanS-dependent vancomycin resistance requires binding of the drug to D-Ala-D-Ala termini in the peptidoglycan cell wall. *Antimicrobial agents and chemotherapy* 57, 4470-4480.
57. Arthur, M., Molinas, C., and Courvalin, P. (1992). The VanS-VanR two-component regulatory system controls synthesis of depsipeptide peptidoglycan precursors in *Enterococcus faecium* BM4147. *Journal of bacteriology* 174, 2582-2591.
58. Nicolaou, K.C., Boddy, C.N., Brase, S., and Winssinger, N. (1999). Chemistry, Biology, and Medicine of the Glycopeptide Antibiotics. *Angew Chem Int Ed Engl* 38, 2096-2152. 10.1002/(sici)1521-3773(19990802)38:15<2096::aid-anie2096>3.0.co;2-f.
59. Xu, M., Wang, W., Waglechner, N., Culp, E.J., Guitor, A.K., and Wright, G.D. (2020). GPAHex-A synthetic biology platform for Type IV-V glycopeptide antibiotic production and discovery. *Nat Commun* 11, 5232. 10.1038/s41467-020-19138-5.
60. Alcorlo, M., Straume, D., Lutkenhaus, J., Havarstein, L.S., and Hermoso, J.A. (2020). Structural Characterization of the Essential Cell Division Protein FtsE and Its Interaction with FtsX in *Streptococcus pneumoniae*. *mBio* 11. 10.1128/mBio.01488-20.

61. Jumper, J., Evans, R., Pritzel, A., Green, T., Figurnov, M., Ronneberger, O., Tunyasuvunakool, K., Bates, R., Zidek, A., Potapenko, A., et al. (2021). Highly accurate protein structure prediction with AlphaFold. *Nature* *596*, 583-589. 10.1038/s41586-021-03819-2.
62. Greene, N.P., Kaplan, E., Crow, A., and Koronakis, V. (2018). Antibiotic Resistance Mediated by the MacB ABC Transporter Family: A Structural and Functional Perspective. *Front Microbiol* *9*, 950. 10.3389/fmicb.2018.00950.
63. Tiwari, S., Jamal, S.B., Hassan, S.S., Carvalho, P., Almeida, S., Barh, D., Ghosh, P., Silva, A., Castro, T.L.P., and Azevedo, V. (2017). Two-Component Signal Transduction Systems of Pathogenic Bacteria As Targets for Antimicrobial Therapy: An Overview. *Front Microbiol* *8*, 1878. 10.3389/fmicb.2017.01878.
64. Cheung, J., and Hendrickson, W.A. (2010). Sensor domains of two-component regulatory systems. *Curr Opin Microbiol* *13*, 116-123. 10.1016/j.mib.2010.01.016.
65. Tierney, A.R., and Rather, P.N. (2019). Roles of two-component regulatory systems in antibiotic resistance. *Future Microbiol* *14*, 533-552. 10.2217/fmb-2019-0002.
66. Pootoolal, J., Neu, J., and Wright, G.D. (2002). Glycopeptide antibiotic resistance. *Annu Rev Pharmacol Toxicol* *42*, 381-408. 10.1146/annurev.pharmtox.42.091601.142813.
67. Wright, G.D., Holman, T.R., and Walsh, C.T. (1993). Purification and characterization of VanR and the cytosolic domain of VanS: a two-component regulatory system required for vancomycin resistance in *Enterococcus faecium* BM4147. *Biochemistry* *32*, 5057-5063. 10.1021/bi00070a013.
68. Holman, T.R., Wu, Z., Wanner, B.L., and Walsh, C.T. (1994). Identification of the DNA-binding site for the phosphorylated VanR protein required for vancomycin resistance in *Enterococcus faecium*. *Biochemistry* *33*, 4625-4631. 10.1021/bi00181a024.
69. Peterson, E., and Kaur, P. (2018). Antibiotic Resistance Mechanisms in Bacteria: Relationships Between Resistance Determinants of Antibiotic Producers, Environmental Bacteria, and Clinical Pathogens. *Front Microbiol* *9*, 2928. 10.3389/fmicb.2018.02928.
70. Higgins, C.F. (1992). ABC transporters: from microorganisms to man. *Annu Rev Cell Biol* *8*, 67-113. 10.1146/annurev.cb.08.110192.000435.
71. George, N.L., Schillmiller, A.L., and Orlando, B.J. (2022). Conformational snapshots of the bacitracin sensing and resistance transporter BceAB. *Proc Natl Acad Sci U S A* *119*, e2123268119. 10.1073/pnas.2123268119.
72. Dintner, S., Heermann, R., Fang, C., Jung, K., and Gebhard, S. (2014). A sensory complex consisting of an ATP-binding cassette transporter and a two-component regulatory system controls bacitracin resistance in *Bacillus subtilis*. *J Biol Chem* *289*, 27899-27910. 10.1074/jbc.M114.596221.
73. Kobras, C.M., Piepenbreier, H., Emenegger, J., Sim, A., Fritz, G., and Gebhard, S. (2020). BceAB-Type Antibiotic Resistance Transporters Appear To Act by Target Protection of Cell Wall Synthesis. *Antimicrob Agents Chemother* *64*. 10.1128/AAC.02241-19.
74. Rich, M.H., Sharrock, A.V., Mulligan, T.S., Matthews, F., Brown, A.S., Lee-Harwood, H.R., Williams, E.M., Copp, J.N., Little, R.F., Francis, J.J.B., et al. (2023). A metagenomic library cloning strategy that promotes high-level expression of captured genes to enable efficient functional screening. *Cell Chem Biol* *30*, 1680-1691 e1686. 10.1016/j.chembiol.2023.10.001.

75. Kieser, T., Bibb, M. J, Buttner M. J, Chater K. F, Hopwood D. A. (2000). Practical Streptomyces Genetics (John Innes Foundation Norwich).
76. Scientific, T. (2017). Thermo Scientific Maxima™ H Minus cDNA Synthesis Master Mix with dsDNase.
77. Lu, S., and Zgurskaya, H.I. (2013). MacA, a periplasmic membrane fusion protein of the macrolide transporter MacAB-TolC, binds lipopolysaccharide core specifically and with high affinity. *J Bacteriol* 195, 4865-4872. 10.1128/jb.00756-13.
78. Capstick, D.S., Jomaa, A., Hanke, C., Ortega, J., and Elliot, M.A. (2011). Dual amyloid domains promote differential functioning of the chaplin proteins during Streptomyces aerial morphogenesis. *Proc Natl Acad Sci U S A* 108, 9821-9826. 10.1073/pnas.1018715108.
79. Bhavsar, A.P., Zhao, X., and Brown, E.D. (2001). Development and characterization of a xylose-dependent system for expression of cloned genes in Bacillus subtilis: conditional complementation of a teichoic acid mutant. *Appl Environ Microbiol* 67, 403-410. 10.1128/AEM.67.1.403-410.2001.
80. Sharpe, A., Blumberg, P.M., and Strominger, J.L. (1974). D-alanine carboxypeptidase and cell wall cross-linking in Bacillus subtilis. *J Bacteriol* 117, 926-927. 10.1128/jb.117.2.926-927.1974.
81. Lavysh, D., Sokolova, M., Slashcheva, M., Forstner, K.U., and Severinov, K. (2017). Transcription Profiling of Bacillus subtilis Cells Infected with AR9, a Giant Phage Encoding Two Multisubunit RNA Polymerases. *mBio* 8. 10.1128/mBio.02041-16.
82. Hong, H.J., Hutchings, M.I., Hill, L.M., and Buttner, M.J. (2005). The role of the novel Fem protein VanK in vancomycin resistance in Streptomyces coelicolor. *J Biol Chem* 280, 13055-13061. 10.1074/jbc.M413801200.
83. Paget, M.S., Chamberlin, L., Atrih, A., Foster, S.J., and Buttner, M.J. (1999). Evidence that the extracytoplasmic function sigma factor ζE is required for normal cell wall structure in Streptomyces coelicolor A3 (2). *Journal of bacteriology* 181, 204-211.

Appendices

Appendix 1 Master Mixes and Media

TSBY broth (1 L, autoclave)

Reagent	Amount	Supplier
Tryptic Soy Broth	30.0g	Fisher Scientific
Yeast Extract	5.0 g	Fisher Scientific

SFM agar (1L, autoclave)

Reagent	Amount	Supplier
Mannitol	20.0 g	Bioshop Canada
Soya Flour	20.0 g	Bulk Barn
Agar	20.0 g	Bioshop Canada

MYM (1L, autoclave)

Reagent	Amount	Supplier
Maltose	4.0 g	Fisher Scientific
Yeast Extract	4.0 g	Fisher Scientific
Malt Extract	10.0 g	Bioshop Canada
Agar	15.0 g	Bioshop Canada

Dissolve ingredients in 500 mL of tap water and 250 mL of ddH₂O, pH to 7.2-7.3 with NaOH. Add ddH₂O to 1 L.

ISP4 broth or agar (1L, autoclave)

Reagent	Amount	Supplier
Soluble Starch	10.0 g	Fisher Scientific
MgSO ₄ x 7H ₂ O	1.0 g	Sigma Aldrich
Sodium Chloride	1.0 g	Fisher Scientific
Ammonium Sulfate	2.0 g	Sigma Aldrich
Calcium Carbonate	2.0 g	Sigma Aldrich
*Agar	20.0 g	Bioshop Canada
**Trace Salts Solution	1 mL	

Bring ingredients except for the Trace Salts solution to pH 7.0-7.4. After autoclave add 1 mL of filter-sterilized Trace Salts to media, mix well.

*optional, only if making plates

** in 100 mL dH₂O

- 0.1 g FeSO₄ x 7H₂O
- 0.1 g MnCl₂ x 4H₂O
- 0.1 g ZnSO₄ x 7H₂O

Bennett's (1L, autoclave)

Reagent	Amount	Supplier
Potato Starch	10.0 g	Bulk Barn
Casamino acids	2.0 g	Bioshop Canada
Yeast Extract	1.8 g	Fisher Scientific
*Agar	1.0 g	Bioshop Canada
**Czapek Mineral Mix	2.0 mL	

pH to 6.8, autoclave as normal.

*optional, only if making plates

** in 100 mL dH₂O

- 10 g KCl
- 10 g MgSO₄ x 7H₂O
- 12 g NaNO₃
- 0.2 FeSO₄ x 7H₂O
- 200 µL concentrated HCl

SAM (1L, autoclave)

Reagent	Amount	Supplier
Glucose	15.0 g	Cedarlane Cedarlane
Soytone	15.0 g	Fisher Scientific
Sodium Chloride	5.0 g	Fisher Scientific

Yeast Extract	1.0 g	Fisher Scientific
Calcium Carbonate	1.0 g	Sigma Aldrich
Glycerol	2.5 mL	Bioshop Canada
*Agar	15.0 g	Bioshop Canada

pH media to 6.8, autoclave as normal.

*optional, only if making plates

ST base (1L, autoclave)

Reagent	Amount	Supplier
Ammonium sulfate	15 mM	Sigma Aldrich
K ₂ HPO ₄	700 mM	Bioshop Canada
KH ₂ PO ₄	45 mM	Bioshop Canada
Sodium Citrate, dihydrate	3.5 mM	Sigma Aldrich

pH to 7.0, autoclave as normal

SM1 (15 mL filter sterilize)

Reagent	Amount	Supplier
ST base	15.0 mL	
Magnesium Sulfate (300 mM)	37.5 µL	Sigma Aldrich
**50X YECA	300 µL	
Tryptophan (10 mg/mL)	150 µL	Sigma Aldrich
Glucose (50%)	150 µL	Cedarlane Cedarlane

** in 50 mL ddH₂O

- 5g Bacto yeast extract
- 0.625g Casamino acids

May need heating at 60°C to fully go into solution, filter sterilize

SM2

Reagent	Amount	Supplier
ST base	15.0 mL	
Magnesium Sulfate (300 mM)	150 µL	Sigma Aldrich
**50X YECA	150 µL	(See SM1)
Tryptophan (10 mg/mL)	150 µL	Sigma Aldrich
Glucose (50%)	150 µL	Cedarlane Cedarlane
Calcium Chloride (300 mM)	75 µL	Sigma Aldrich

TfBI (dissolved in water, filter sterilized and stored at 4°C)

Reagent	Amount	Supplier
Potassium Acetate	30 mM	Cedarlane Cedarlane
Rubidium Chloride	100 mM	Bioshop Canada
Calcium Chloride	10 mM	Sigma Aldrich
Manganese Chloride	50 mM	Bioshop Canada
Glycerol	15% (v/v)	Bioshop Canada
Dilute acetic acid	Enough to reach pH of 5.8	Bioshop Canada

TfBII (dissolved in water, filter sterilized and stored at 4°C)

Reagent	Amount	Supplier
MOPS	10 mM	Bioshop Canada
Rubidium Chloride	100 mM	Bioshop Canada
Calcium Chloride	75 mM	Sigma Aldrich
Glycerol	15% (v/v)	Bioshop Canada
Sodium Hydroxide	Enough to reach pH of 6.5	Bioshop Canada

Solution I Cosmid preparation (100 mL)

Reagent	Amount	Supplier
Glucose	50 mM	Cedarlane Cedarlane
Tris-HCl (pH 8)	25 mM	Bioshop Canada
EDTA	10 mM	Fisher Scientific

Solution II Cosmid preparation (50 mL)

Reagent	Amount	Supplier
Sodium Hydroxide	200 mM	Bioshop Canada
SDS	1% (m/v)	Bioshop Canada

Solution III Cosmid preparation (100 mL, keep at 4°C)

Reagent	Amount	Supplier
Potassium Acetate (3 M)	60 mL	Cedarlane Cedarlane
Glacial Acetic Acid	11.5 mL	Bioshop Canada

Add ddH₂O to 100 mL.

50X TAE buffer

Tris base 242 g (BioShop)

Acetic acid 57.1 mL (Caledon)

EDTA 37.2 g (Fisher)

To 1 L of dH₂O Gels are made with 1X TAE buffer.**6X DNA loading dye**

0.25% Bromophenol Blue (2 mg) (300 bp)

30% glycerol in dH₂O (3mL + 7 mL dH₂O)

0.25% xylene (4kb) 5-Bromo-n-xylene, (Sigma)

Appendix 2 Primers**Chapter 2**

Primer name	Sequence	Ref
EnC-RC-pIJ	Fwd 5' <i>ACAGTACCATATGTTTCACCACACGCAAACG</i> Rev 5' <i>ACAGTACAAGCTTCGTTCCGCTCACCAGTCC</i>	This study
Enu-RC-pIJ	Fwd 5' <i>ACAGTACCATATGTTTCACCACACGCAAACG</i> Rev 5' <i>ACAGTACAAGCTTGTACGTCAGGTGGTGGCC</i>	This study
COM-RC-pIJ	Fwd 5' <i>ACAGTACCATATGTTCTCCACACAACGACGTG</i> Rev 5' <i>ACAGTACAAGCTTCTTGCGGGGGATTTTCGAGG</i>	This study
EnC-col	Fwd 5' <i>AAACCCTTCGCCTTCGCC</i> Rev 5' <i>TTCGATCAGCCGCTCCTG</i>	This study
Enu-col	Fwd 5' <i>AGGTCGAACTGCCCAACG</i> Rev 5' <i>GATGACGACGACGGTGGT</i>	This study

COM-col	Fwd 5' CTCAACGCCGAGGAGACC Rev 5' CGGGGTGCTGCTGTAGAG	This study
EnuS-RT	Fwd 5' GGTACGGATCATGGCGGG Rev 5' GTCGCCGAGGTCCTTCAG	This study
EnuR-RT	Fwd 5' GCAGCGAGTACGACGTGA Rev 5' GGTGATGGAGGCGGTGAG	This study
EnuU-RT	Fwd 5' GCGGGCGTCATGTTCAAC Rev 5' CGCGACCTTCTCGGAGTC	This study
EnuP-RT	Fwd 5' AGGTCGAACTGCCCAACG Rev 5' CAGCGTGGACTCCTGGTC	This study
EnuE-RT	Fwd 5' CTCTACCACGAGCCGCAC Rev 5' AGCAGCTCCATCACGACC	This study
EnuX-RT	Fwd 5' CAGTCGTTCTCGGGCTCC Rev 5' GTTGCGGAAGACGTTGGC	This study
ComT-RT	Fwd 5' TCAACGGCGGTCAGATGG Rev 5' ATCATCATCCCGCCACCG	This study
ComS-RT	Fwd 5' GGGCAAGGTCACCGACAT Rev 5' ATCTCGAGCTGGACCGGA	This study
ComR-RT	Fwd 5' CTCTACAGCAGCACCCCG Rev 5' CTTCTCACCGCCGGAGAG	This study
ComQ-RT	Fwd 5' GCATCTCGACGTCCAGCA Rev 5' CATCTGCACCGACTCGCT	This study
hrdB-Sven-RT	Fwd 5' GATCCGCCGCCAAGAAGA Rev 5' TCGTCGGCGTCCTTCTTG	This study

Chapter 3

Primer name	Sequence	Ref
EnC-RC-pSWE	Fwd. 5' <i>ACAGTACTTAATTAATCTGTATCCGCCCTGTGAC</i> Rev 5' <i>ACAGTACGCTAGCCGTTCCGCTCACCAGTCC</i>	This study

Enu-RC-pSWE	Fwd 5' <i>ACAGTACTTAATTAATCTGTATCCGCCCTGTGAC</i> Rev 5' <i>ACAGTACGCTAGCGTACGTCAGGTGGTGGCC</i>	This study
COM-RC-pSWE	Fwd 5' <i>ACAGTACCATATGTTCTCCACACAACGACGTG</i> Rev 5' <i>ACAGTACAAGCTTCTTGCGGGGGATTTTCGAGG</i>	This study
EnC-col	Fwd 5' <i>AAACCCTTCGCCTTCGCC</i> Rev 5' <i>TTCGATCAGCCGCTCCTG</i>	Ch. 2
Enu-col	Fwd 5' <i>AGGTCGAACTGCCCAACG</i> Rev 5' <i>GATGACGACGACGGTGGT</i>	Ch. 2
COM-col	Fwd 5' <i>CTCAACGCCGAGGAGACC</i> Rev 5' <i>CGGGGTGCTGCTGTAGAG</i>	Ch. 2
EnuS-RT	Fwd 5' <i>GGTACGGATCATGGCGGG</i> Rev 5' <i>GTCGCCGAGGTCCTTCAG</i>	Ch. 2
EnuR-RT	Fwd 5' <i>GCAGCGAGTACGACGTGA</i> Rev 5' <i>GGTGATGGAGGCGGTGAG</i>	Ch. 2
EnuU-RT	Fwd 5' <i>GGCGGCGTCATGTTCAAC</i> Rev 5' <i>CGCGACCTTCTCGGAGTC</i>	Ch. 2
EnuP-RT	Fwd 5' <i>AGGTCGAACTGCCCAACG</i> Rev 5' <i>CAGCGTGGACTCCTGGTC</i>	Ch. 2
EnuE-RT	Fwd 5' <i>CTCTACCACGAGCCGCAC</i> Rev 5' <i>AGCAGCTCCATCACGACC</i>	Ch. 2
EnuX-RT	Fwd 5' <i>CAGTCGTTCTCGGGCTCC</i> Rev 5' <i>GTTGCGGAAGACGTTGGC</i>	Ch. 2
ComT-RT	Fwd 5' <i>TCAACGGCGGTCAGATGG</i> Rev 5' <i>ATCATCATCCCGCCACCG</i>	Ch. 2
ComS-RT	Fwd 5' <i>GGGCAAGGTCACCGACAT</i> Rev 5' <i>ATCTCGAGCTGGACCGGA</i>	Ch. 2
ComR-RT	Fwd 5' <i>CTCTACAGCAGCACCCCG</i> Rev 5' <i>CTTCTCACCGCCGGAGAG</i>	Ch. 2
ComQ-RT	Fwd 5' <i>GCATCTCGACGTCCAGCA</i> Rev 5' <i>CATCTGCACCGACTCGCT</i>	Ch. 2

yoxA	Fwd 5' CCTTTGTTTCATGACCGTCGC Rev 5' TCCCCATGTGCAGAAGCAAT	81
Cod-opt-Frag1	Fwd 5' GTGCTTTAGTTGAAGAATAAAGACCGCTAG Rev 5' CTTTCACTAAATCTTCATGTTGAGGATCAAG	This study
Cod-opt-Frag2	Fwd 5' CTTTCACTAAATCTTCATGTTGAGG Rev 5' GTGCTTGAATACAGTAGACCATCTG	This study
Cod-opt-Frag3	Fwd 5' CAGATGGTCTACTGTATTCAAGCAC Rev 5' CAACTGGTAATGGTAGCGAC	This study
Cod-opt-PSWE	Fwd 5' GTCGCTACCATTACCAGTTG Rev 5' GGTCTTTATTCTTCAACTAAAGCAC	This study
Cod-opt-Frag1 w/xyl	Fwd 5' ATGTTTTCTACCCAGCGCCGT Rev 5' CTTTCACTAAATCTTCATGTTGAGGATCAAG	This study
Cod-opt-PSWE w/xyl	Fwd 5' GTCGCTACCATTACCAGTTG Rev 5' TTAAAGAAACGCTCCTTCCTAATG	This study

Appendix 3 Plasmid Maps

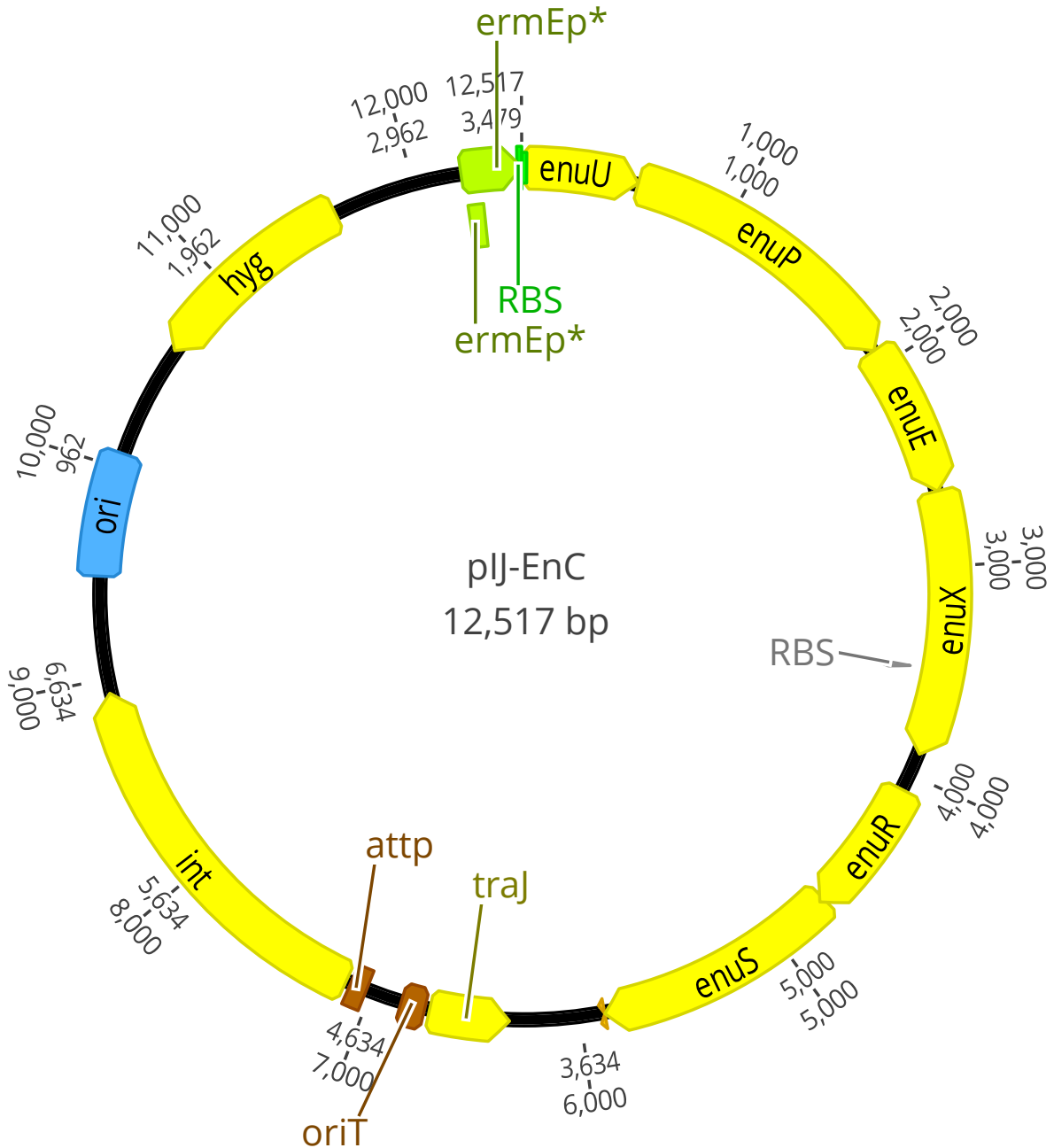


Figure S1. pIJ10257 is used as the backbone for pIJ-EnC. The pIJ10257 plasmid was first described in Hong et al.⁸² pIJ-EnC contains the putative resistance cassette including the two-component system from the muobactin-producer WAC06738. The antibiotic selection marker for this plasmid is hygromycin. It also possesses conjugation machinery to be chromosomally integrated into *Streptomyces* species at the Φ BT1 phage integration site and a strong constitutive promoter *ermE**.

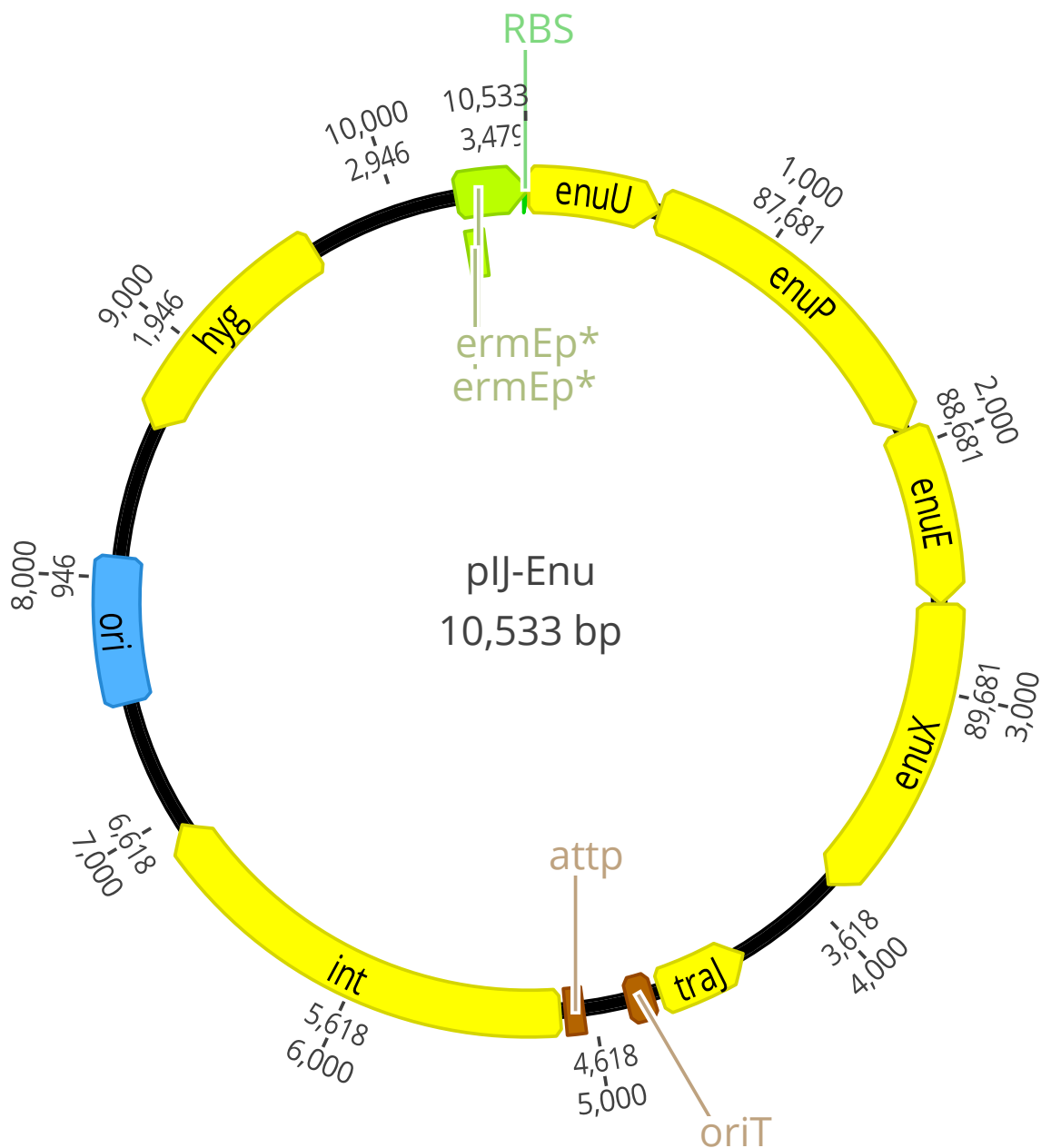


Figure S2. pIJ10257 is used as the backbone for pIJ-Enu. The pIJ10257 plasmid was first described in Hong et al.⁸² pIJ-Enu contains the putative resistance core not including the two-component system from the muobactin-producer WAC06738. The antibiotic selection marker for this plasmid is hygromycin. It also possesses conjugation machinery to be chromosomally integrated into *Streptomyces* species at the Φ BT1 phage integration site and a strong constitutive promoter *ermE**.

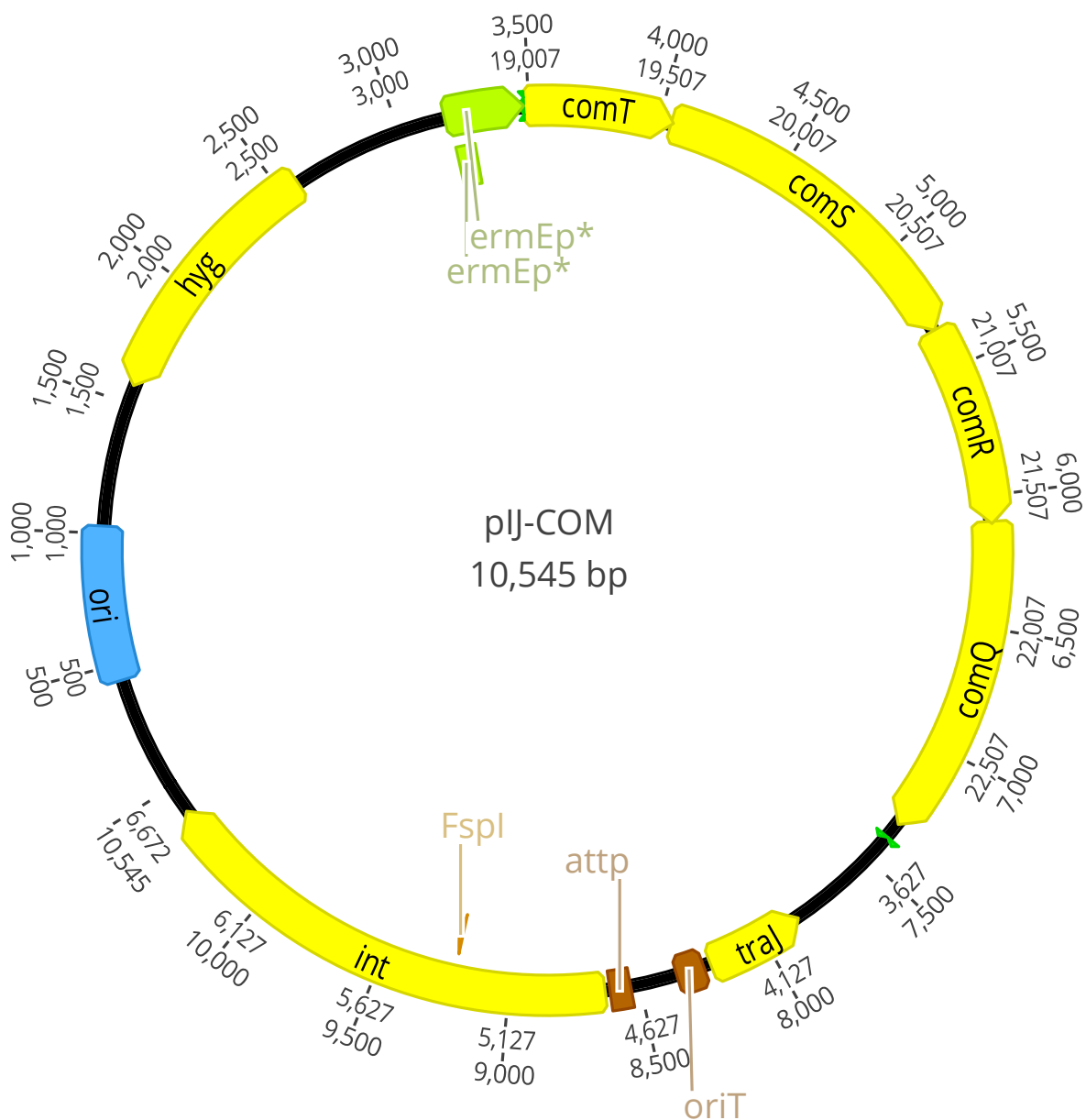


Figure S3. pIJ10257 is used as the backbone for pIJ-Enu. The pIJ10257 plasmid was first described in Hong et al.⁸² pIJ-Enu contains the putative resistance core not including the two-component system from the muobactin-producer WAC01325. The antibiotic selection marker for this plasmid is hygromycin. It also possesses conjugation machinery to be chromosomally integrated into *Streptomyces* species at the Φ BT1 phage integration site and a strong constitutive promoter *ermE**.

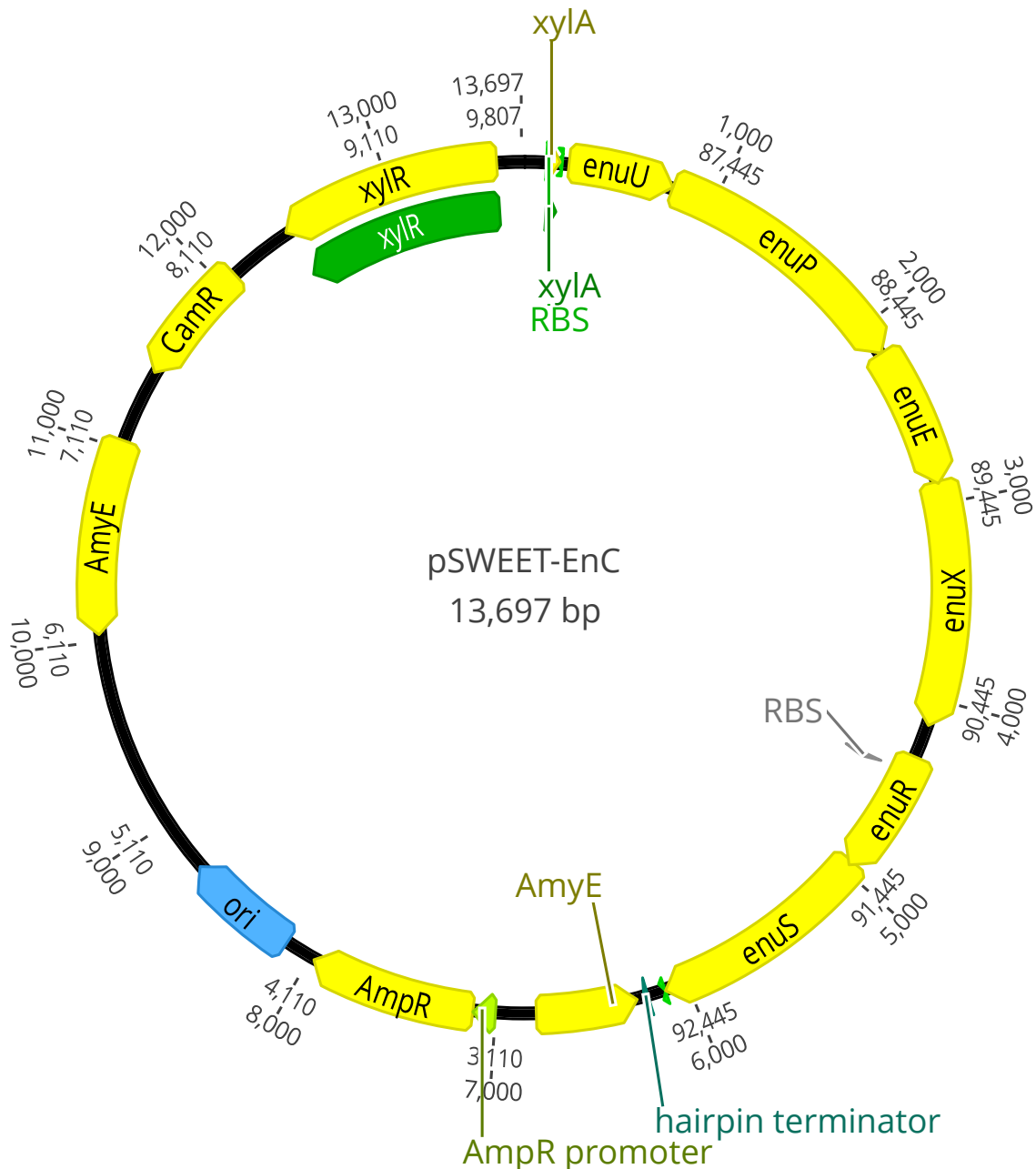


Figure S4. pSWEET-bgaB was used as the backbone for pSWEET-EnC. The pIJ10257 plasmid was first described in Bhavsar et al.⁷⁹ pSWEET-EnC contains the putative resistance cassette including the two-component system from the murobactin-producer WAC06738. The antibiotic selection markers for this plasmid are ampicillin and chloramphenicol. It also possesses a xylose-dependent expression system and can be integrated into the chromosome due to amyE sites.

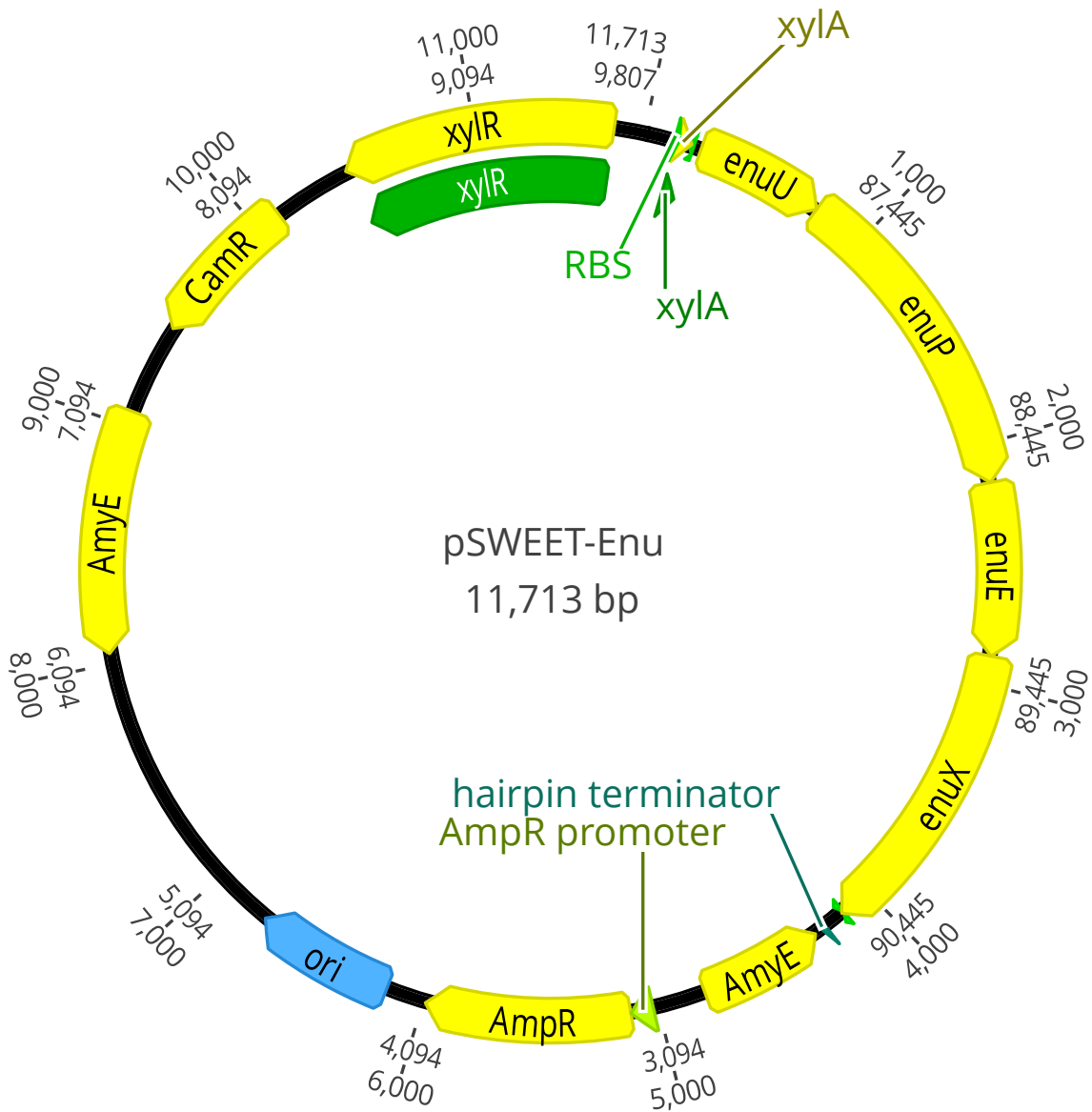


Figure S5. pSWEET-bgaB was used as the backbone for pSWEET-Enu. The pIJ10257 plasmid was first described in Bhavsar et al.⁷⁹ pSWEET-Enu contains the putative resistance core not including the two-component system from the muobactin-producer WAC06738. The antibiotic selection markers for this plasmid are ampicillin and chloramphenicol. It also possesses a xylose-dependent expression system and can be integrated into the chromosome due to amyE sites.

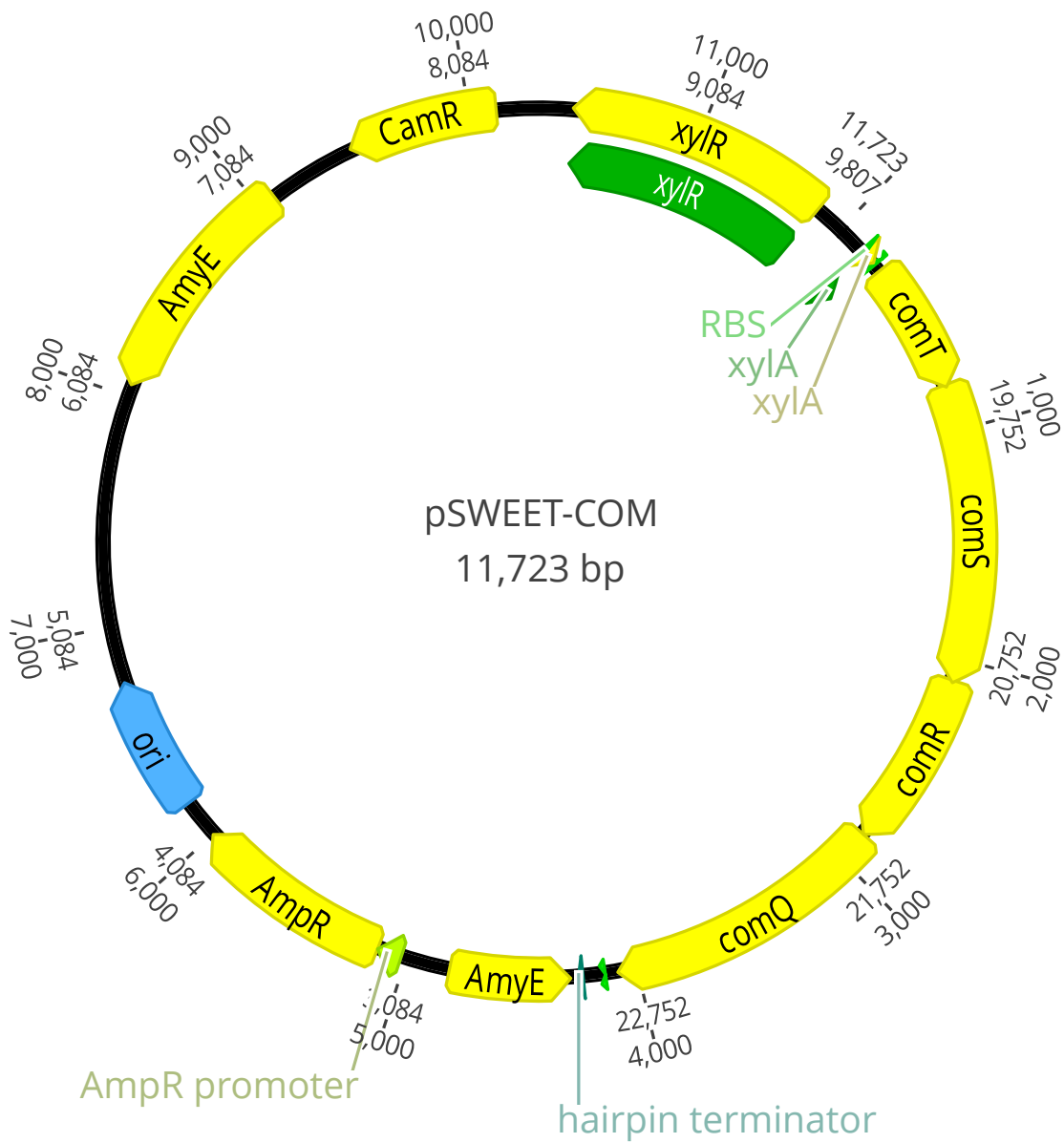


Figure S6. pSWEET-bgaB was used as the backbone for pSWEET-COM. The pIJ10257 plasmid was first described in Bhavsar et al.⁷⁹ pSWEET-COM contains the putative resistance core not including the two-component system from the murobactin-producer WAC01325. The antibiotic selection markers for this plasmid are ampicillin and chloramphenicol. It also possesses a xylose-dependent expression system and can be integrated into the chromosome due to amyE sites.

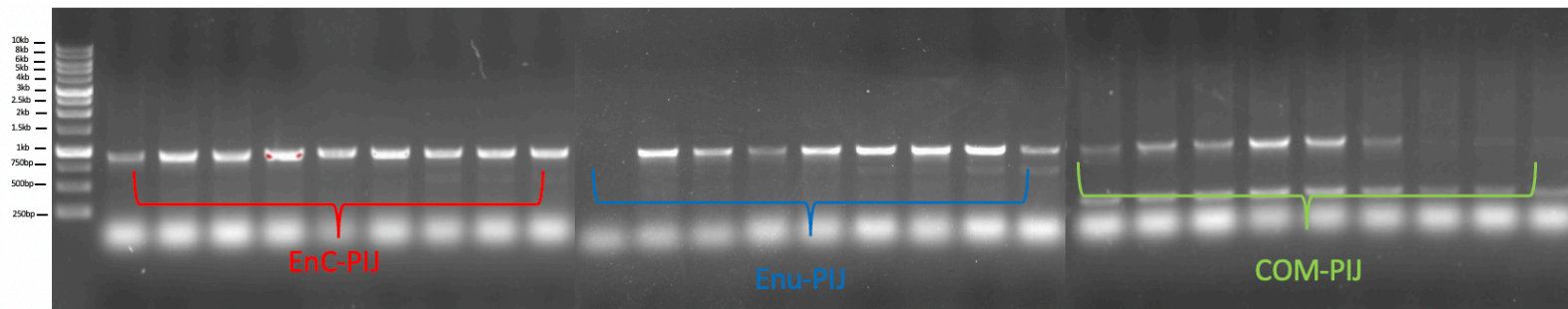


Figure S9. Electrophoresis gels of chromosomal integration of putative resistance cassette. Genomic DNA was isolated from *S. coelicolor* exconjugants. Colony PCR primers were used to assess integration. Each exconjugant PCR was done in triplicate, only strains with all positive hits were made into spore stocks.

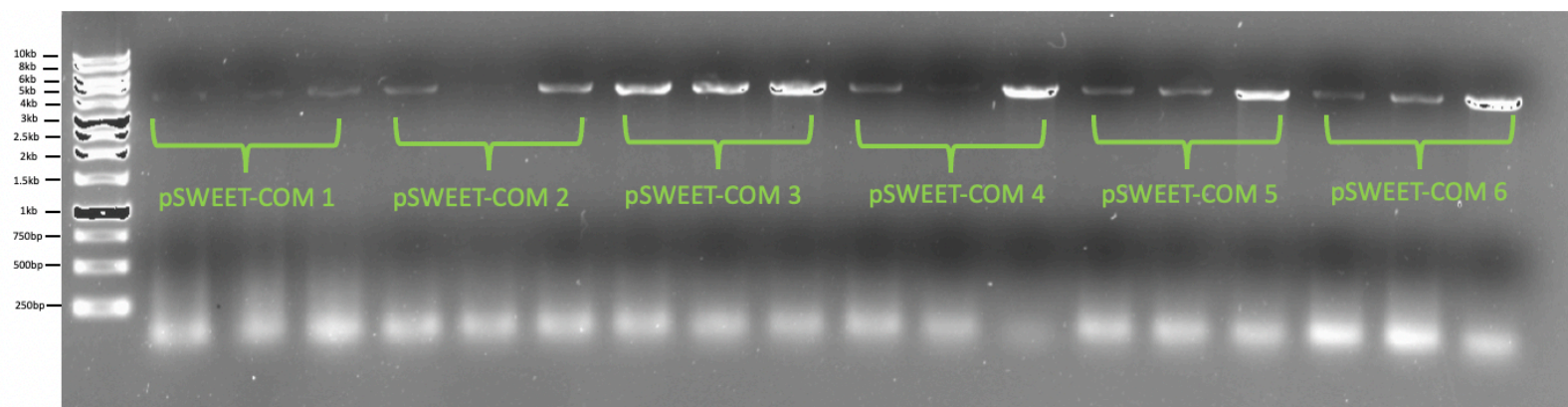


Figure S10. Electrophoresis gels of chromosomal integration of putative resistance cassette. Genomic DNA was isolated from *B. subtilis* transformants. Colony PCR primers were used to assess integration. Each transformant PCR was done in triplicate, only pSWEET-COM 3 was continued for experimental use.